creative commons
COMMONS DEED

저작자표시-비영리-변경금지 2.0 대한민국

이용자는 아래의 조건을 따르는 경우에 한하여 자유롭게

- 이 저작물을 복제, 배포, 전송, 전시, 공연 및 방송할 수 있습니다.

다음과 같은 조건을 따라야 합니다:

저작자표시. 귀하는 원저작자를 표시하여야 합니다.

비영리. 귀하는 이 저작물을 영리 목적으로 이용할 수 없습니다.

변경금지. 귀하는 이 저작물을 개작, 변형 또는 가공할 수 없습니다.

- 귀하는, 이 저작물의 재이용이나 배포의 경우, 이 저작물에 적용된 이용허락조건을 명확하게 나타내어야 합니다.
- 저작권자로부터 별도의 허가를 받으면 이러한 조건들은 적용되지 않습니다.

저작권법에 따른 이용자의 권리는 위의 내용에 의하여 영향을 받지 않습니다.

이것은 이용허락규약(Legal Code)을 이해하기 쉽게 요약한 것입니다.

Disclaimer

dCollection

[UCI]I804:48009-200000107941

공학석사 학위논문

A Study on the Strengthening of Cold Punch Mold Using Metal Powder (Mold Steel and High Speed Tool Steel) and DED AM Technology

금속 분말 (금형강 및 고속 공구강)과 DED AM 기술을 이용한 냉간 펀치 금형의 강화에 관한 연구

울산대학교 대학원

기계자동차공학과

이예

금속 분말 (금형강 및 고속 공구강)과 DED AM 기술을 이용한 냉간 펀치 금형의 강화에 관한 연구

지도교수 양 순 용

이 논문을 공학석사 학위 논문으로 제출함

2018 년 5 월

울산대학교 대학원

기계자동차공학과

이예

A Study on the Strengthening of Cold Punch Mold Using Metal Powder (Mold Steel and High Speed Tool Steel) and DED AM Technology

Advisor: Professor Soon Yong Yang

Submitted to the Office of Graduate School of
University of Ulsan
In partial Fulfillment of the Requirements for the Degree of

Master of Science

By

Rui Li

School of Mechanical Engineering

University of Ulsan

Ulsan, Republic of Korea

May 2018

이예의 공학석사학위 논문을 인준함

심사위원 염 영 진 인

심사위원 김 용 석 인

심사위원 양 순 용 인

울산대학교 대학원

2018년 05월

A Study on the Strengthening of Cold Punch Mold Using Metal Powder (Mold Steel and High Speed Tool Steel) and DED AM Technology

This certifies that the master's thesis of Rui Li is approved by

_____

Committee Chair Prof. Young Jin Yum

_____

Committee Member Prof. Yong Seok Kim

_____

Committee Member Prof. Soon Yong Yang

ACKNOWLEDGEMENTS

The completion of the thesis is attributed to many peoples support and encouragement.

Sincerely, I am very grateful to my professors for guidance, Prof. Young Jin Yum Prof. Yong Seok Kim Prof. Soon Yong Yang. Their conscientious academic spirit and modest, open-minded personality inspire me both in academic study and daily life.

Second, I am honored to meet the brothers in our laboratory.

Last but not least, I would like to express my special thanks to my family, whose care and support motivate me to move on and make me want to be a better person.

ABSTRACT

In this paper, the aim of it is to create additive manufacturing fabrication for high-strength punches. In order to deal with the high-strength parts of the vehicle, it was confirmed that a full-additive manufacturing punch could be fabricated by cold punch mold metal powder materials (mold steel or high speed tool steel) using the 3D printing technology. For the manufacturing method, the analysis of the DED (Directed energy deposition) will be performed compare with other method of additive manufacturing method. Based on the previous studies, it can be seen that HWS powder metal material exhibits better mechanical properties in many powder materials such as M4, M300 and so on. Therefore, in this article, we focused on the performance of HWS powder metal material. The comparative specimens were produced by bulk materials of bulk D2 and bulk HWS. In order to obtain the better mechanical properties of the powder material, there is a post process for the additive manufacturing specimens which used the heat treatment after fabrication by additive manufacturing. In the experimental section, it was designed according to experimental principles and test standards. The problems in the experimental process and the evaluation indicators of the experimental results will be presented in this study. From the results of the experiment, the specimens produced by the additive manufacturing fully demonstrate the mechanical properties of the material. A material of HWS has an excellent mechanical property with the comparison of the test results. The results show that HWS has better mechanical properties and the possibility of replacing bulk materials to fabricate punch. In addition to this, various semi-additive manufacturing punch shapes are simulated and analyzed in order to select the partial shape for reinforcement of the piercing punch. After analyzing the simulation results, it was found that the shape of the flat type is the most stable,

and it has been found that the shape of the edge having a triangular sectional shape is stable. The semi-additive shape selected by this simulation will be used to intensify punches which fabricated by using metal powder and AM technology. In the future, the more simulation software was used for mechanical analysis of the punch during the stamping process. Laminated combination of multiple materials will be tested in order to achieve more excellent mechanical properties. Moreover, additive manufacturing punch should test the durability and wear resistance. The quality of punching should also be considered as an analysis indicator for the punch.

Keywords: Strengthening punch mold; Punch strength prediction; Semi-additive punch; Directed energy deposition (DED); Metal powder material; Mechanical properties; Additive manufacturing (AM)

CONTENTS

LIST OF FIGURES

LIST OF TABLES

Chapter 1 Introduction

Nowadays, the vehicle lightweight technology requires ultrahigh strength parts that become stronger, which could maintain high safety with only a small amount of materials and minimize the manufacturing cost. It is mainly applied to the field of the vehicle body, as introduced in Figure 1.1 [1]. At the same time, the lighter weight of vehicle components also increases fuel efficiency, which reduces emissions and protects the environment. For the lightweight of the vehicle, the ultra-high-strength steels played a leading role in the automotive production.

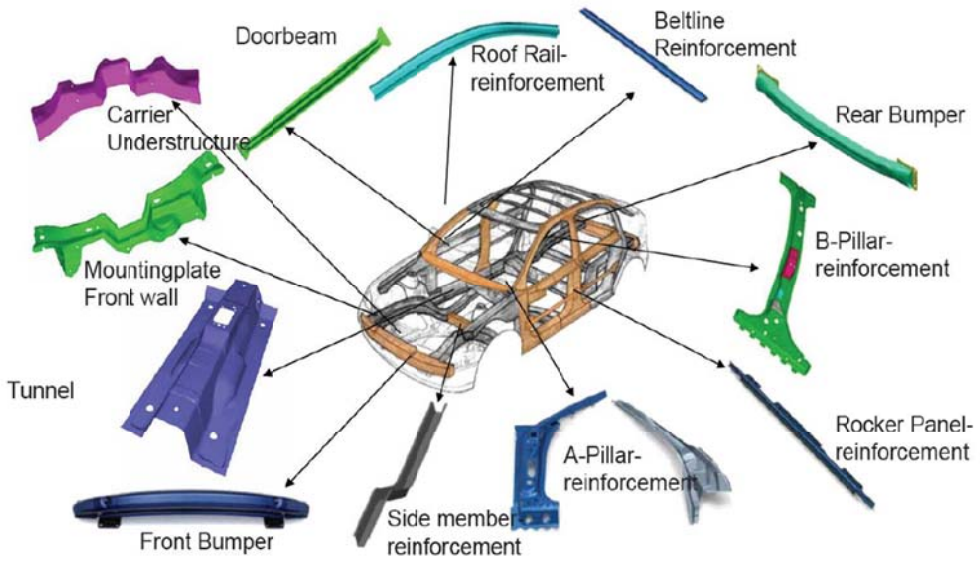

Fig. 1.1 High strength components of the vehicle

1.1 Hot stamping

The position of the technology which is important for reducing the weight of the vehicles would be the hot stamping molding technology. In the hot stamping molding technology, the strength of the materials would be twice as the material before. The effect of light weight would be increased by 25% through cooling channel immediately after heating the sheet material at a constant temperature as mentioned above. There are some advantages that these hot stamping techniques can ensure high safety even with a few materials and enjoy a chain effect such as reduction in manufacturing cost as well as improvement in fuel efficiency because of the reduction in weight and environmental protection by fuel saving. It is mainly applied to the field of the vehicle body, as introduced in Table 1.1. Many famous automobiles in the world are increasingly spread. Thus, despite technical demands and advantages of hot stamping, one of the disadvantages is that it is difficult in the post-processing steps (piercing or trimming) of parts with increasing strength after hot stamping. Currently, most processing stages after hot stamping are solved using laser processing equipment. In the method, a large number (at least three) of expensive laser equipment are required for each process line. In addition, when there are pluralities of work parts for one part, the batch work is difficult and the productivity is lowered. In order to improve these hot-stamping post processes, it could be solved by introducing a press process. However, there are some problems in introducing the press process. The biggest problem is to secure the strength of the mold that can cope with the shear of super high strength parts.

Table 1.1 Hot stamped TRB application in various vehicles. [2]

SOP	Make/Model	Hot Stamped TRB Application
2006	BMW X5	B-Pillar, 5 thicknesses: 1.2 to 2.2 mm, saved 4 kg
2006	Dodge Caliber	B-Pillar, 4 thicknesses: 1.0 to 1.9 mm
2006	JeepPatriot & Compass	B-Pillar, 4thicknesses: 1.09 to 1.95 mm
2007	Mercedes C	Rear bumper, 3 thicknesses, saved 2 kg
2008	BMW X6	B-Pillar, 4 thicknesses: 1.2 to 2.2 mm, saved 4 kg
2010	Volvo S60	Cantrail, saved 3 kg
2011	Audi A6	Cowl beam, 4thicknesses:1.0to1.75 mm
2011	Ford Focus	B-Pillar, 8 thicknesses:1.35 to 2.7mm, saved 1.4 kg
2012	Audi A3	Heel piece, 7 thicknesses: 0.95 to 1.7 mm
2012	BMW 3	B-Pillar, 3 thicknesses: 2.4 to 2.9 mm, saved 1.3 kg
2012	VW Golf	B-Pillar, 3 thicknesses: saved 4 kg

But in the post-manufacturing process of an ultra-high-strength steel sheet such as a hot stamping part manufacturing process, mold damage has become the biggest problem. In order to solve this problem, the current factory uses a laser process. But the laser equipment costs are high and the production efficiency is low. Another solution is to use mold surface treatment. But the deep and strong heat treatment will cause the mold chipping [3].

1.2 Heat treatment

Heat treatment refers to a metal thermal processing process in which the material is in the solid state. It includes three steps about heating, heat preservation, and cooling to obtain the desired structure and properties. The surface heat treatment is a metal heat treatment

process that changes the mechanical properties of the surface by heating and cooling the steel surface. Surface quenching is the main content of surface heat treatment. Its purpose is to obtain high hardness surface layer and favorable internal stress distribution to improve the wear resistance and fatigue resistance of the work piece. In this paper, the method of heat treatment for bulk punches is abandoned because of the strong surface heat treatment that will cause the punch to break. Ordinary heat treatment methods do not reach ideal conditions either. However, heat treatment technology has not been abandoned in additive manufacturing method. It can also be applied to punches after additive manufacturing. So the AM heat treatment punch also serves as a test punch. In this paper, the technology of heat treatment is from ROVALMA. For tempering, immediately after the hardening, when the piece has cooled down to room temperature, start with the tempering cycle.

For high wear resistance, the steps were shown in Figure 1.2. After tempering process, the expected hardness is 62-64 HRc. For high toughness, the steps were shown in Figure 1.3. The expected hardness is 60-62 HRc.

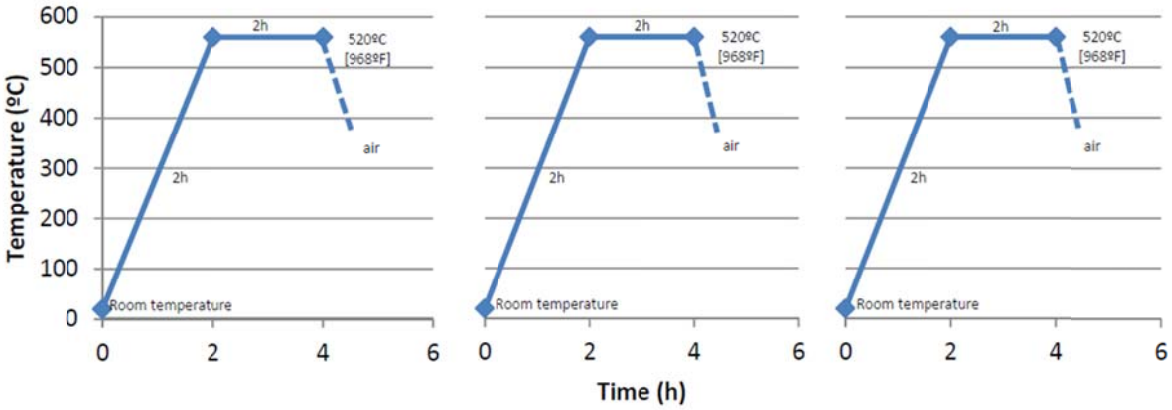

Fig. 1.2 Graph of the recommended tempering process for high wear resistance

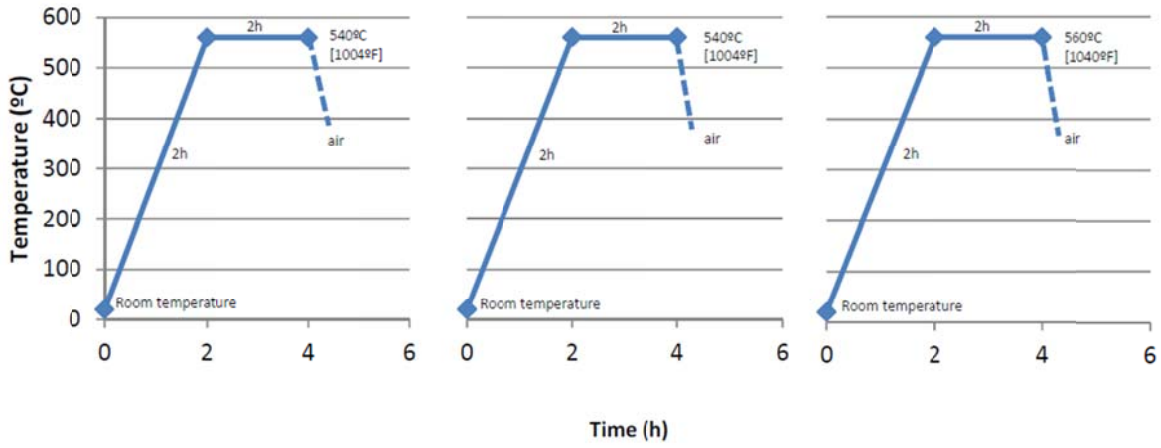

Fig. 1.3 Graph of the recommended tempering process for high toughness

1.3 Additive manufacturing

In view of the development of additive manufacturing technology and the existing achievements, researchers try to use different metal powders and different manufacturing methods to improve the mold's mechanical properties and wear resistance [4-6]. In recent years, Kim et al. provided various characteristics of the products which were fabricated by DMT(Direct Metal Tooling) with the commercial steel powders such as P20, P21, SUS420, H13, D2 and other non-ferrous metal powders, aluminum alloys, titanium alloys, copper alloys and so on [7,8]. Do-Sik Shim et al. studied the effects of process parameters and the mechanical characteristics which were beneficial in reducing the crack susceptibility. In his research, it gives us a guideline for practical hard facing applications which use the high strength metal powders and DED (Direct Energy Deposition) method to improve the performances of the die and mold in wear resistance and toughness [9,10]. Pleterski, M. et al. have been tested metallographic observations and sliding wear to confirm that the AISI D2 tool punches were which cladded by Type-C pulse and manufactured by various laser pulse

shapes, preheating and cryogenic treatment were successfully put back into application [11]. Park et al. studied the effect of heat treatment on the tool steel materials of H13 and D2 by DED (Direct Energy Deposition) method from comparison with the deposited tool steel before and after heat treatment through the test of hardness and microstructure [12]. Also, in the area of AM (Additive Manufacturing), new applications and emerging markets have also emerged as new processes, new technologies, new materials, and increasingly complex and powerful systems emerge including construction, aerospace, medical and automotive industries [13]. The researchers' results demonstrate the possibility of using additive manufacturing to increase the strength of the punch. This also serves as a reference and a starting point for our research.

1.4 Semi-additive manufacturing punch

Currently, punches made by using powder metal and 3D printing technology are very weak in productivity and price competitiveness. This article defines the partially additive manufacturing punch which is called semi-additive manufacturing punch. Because the full additive manufacturing punch is very expensive, it is reflected in the price of the material and the price of the equipment. So, the way to manufacturing semi-additive punch is an important solution to save materials and reduce costs. Semi-additive punches are based on bulk punches for post-processing. However, the shape of the partial additive manufacturing parts has become the biggest problem. So, analyzing the shape of the additive manufacturing section has become a basic requirement. Moreover, semi-additive punch can regenerate low strength punches and damaged punches. So in this paper, we predict the force range of the punch and design a variety of semi-additive punch shape solutions. After using DEFORM simulation, the excellent shape will be selected to manufacture the semi-additive punch.

1.5 Previous research

In previous research of our research, in order to deal with the high-strength parts of the vehicle, it was confirmed that a full-additive manufacturing punch could be fabricated by high strength mold steel powder material using the 3D printing technique [14]. And, the prediction of punch shape range was proposed for improving punch strength by partial semi-additive method using metal 3D printing technique [15]. In previous research and analysis, three kinds of metal powder of H13 M300 and KP4 with excellent additive composition were selected from metal powder materials. The additive manufacturing specimens and punches were produced by PBF (Powder Bed Fusion) method. Then, the specimens of the additive manufacturing were performed in hardness test, the density test and Charpy impact test. Also, the durability of the full-additive punch fabricated would be tested in the piercing press process for high strength sheet material after post treatment. M300 was finally selected as the metal powder material for manufacturing the punch with the analysis of SEM, EDS and mechanical properties. The full-additive manufacturing punches were fabricated by M300 powder material and PBF 3D printing method. In the 10,000 stamping process, the additive-manufactured M300 punch showed the same performance as the SKD-11 and HWS. But the damage was seen on the edge of the M300 punch as shown in Figure 1.4. There are different degrees of glitches appearing on sheet material as shown in Figure 1.5. From the results, the additive manufacturing punch didn't reach a practical standard. So, the use of other types of additive manufacturing method and metal materials is proposed [16].

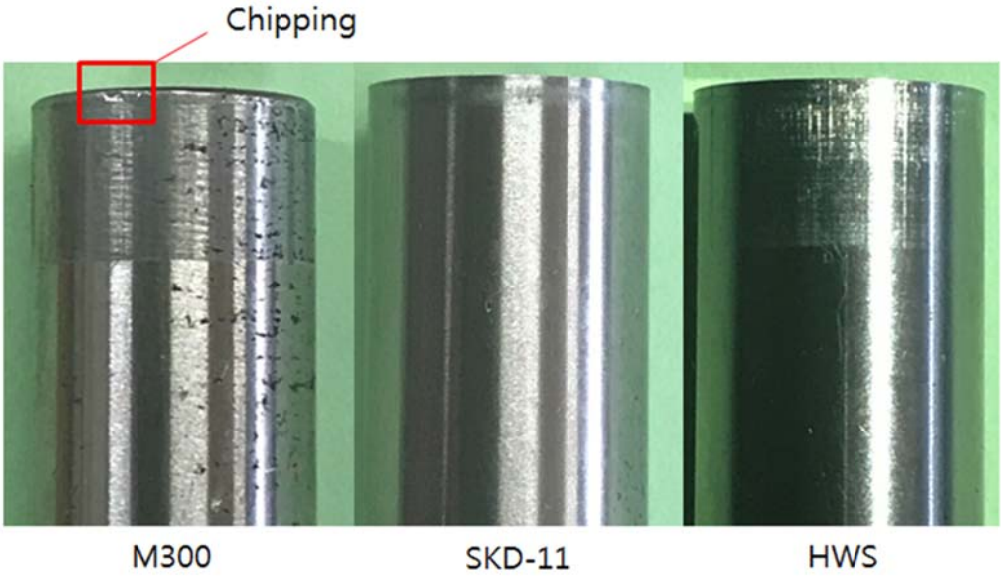

Fig. 1.4 Punch condition after punching test: (a) additive punch of M300 powder material, (b) comparative punch of SKD11 bulk material, (c) comparative punch of HWS bulk material

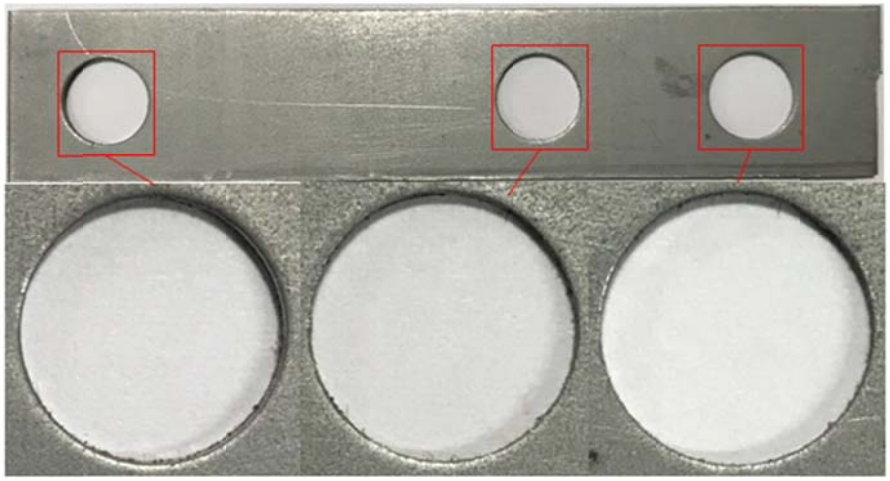

(a) (b) (c)

Fig. 1.5 Sheet specimen condition after punching test with additive and comparative punch: (a) holes shape by additive punch, (b), (**c**) holes shape by comparative punch of SKD-11and HWS

Chapter 2 Additive manufacturing method

2.1 DED method

Directed Energy Deposition (DED) is a 3D printing technology used to create 3D models from metals and alloys [17]. DED is a very important additive manufacturing method for metallic materials. It uses metal powder or metal wire as the raw material, and directly melts the metal on the substrate to form a stacking layer under the action of a high-energy heat source, thereby completing the rapid prototyping of parts. At present, the metal direct deposition manufacturing process can be divided into Laser Engineered Net Shaping (LENS), electron beam fuse deposition manufacturing (EBF) and Wire Arc additive manufacturing (WAAM). The advantage of it is possible to make excellent quality products by perfect fusion between materials. AM products have a dense structure, which is suitable for making tools such as molds. But the disadvantage of it is the high cost and low efficiency. It should take a long time, and the surface to be printed is coarse [18].

The process of DED is similar to the process of material extrusion. However, in the DED printing method, nozzles for supplying material particles or wires are mounted on the multi-axis arm. Thus, the feed is not limited to a particular axis compared to material extrusion. The model is built on the surface from bottom to top. The nozzle for supplying the wire or powder may project the supply from any angle onto the target surface because the multi-axis arm allows movement in four or five axes. The laser beam or laser is directed towards the metal powder immediately. It is deposited on the target surface. The shape of the model is controlled by controlling the feed rate and the angle at which the wire or powder deposits on the structure surface. The material is initially deposited on the substrate. As the deposit cools, a new layer of deposition is deposited on the upper layer, which accumulates

parts one layer by layer.

DED equipment is developed from DMT (Direct Metal Tooling) MX3 metal printing equipment developed by Insstek (Korea) Co., Ltd. The schematic is shown in Figure 2.1. The equipment is built up by a laser heat source, numerical control system, five axis NC machine tool, powder feeding system and corresponding software system. For this equipment, it uses a TRUMP TLF 4000 with a maximum output of 2kW, the beam diameter of 0.8 to 1.0mm and a laser of 4kW CO_2. Numerical control system includes industrial operation computer, tilting and rotating device. The five axis NC machine tool includes X, Y, Z, tilt and rotation. A powder feeding system is consisted of three hoppers and a coaxial powder nozzle. Software system is MX-CAM software.

The track moves back and forth in a fixed direction. The beam spot diameter was 1.0mm with a top-hat intensity distribution. Overlapping tracks have a pitch of 0.5mm. Argon is used as a shielding gas. The machining head with concentric powder is integrated with the optical system to supply powder coaxially with the laser beam to the substrate surface which is 9 mm away from the nozzle tip.

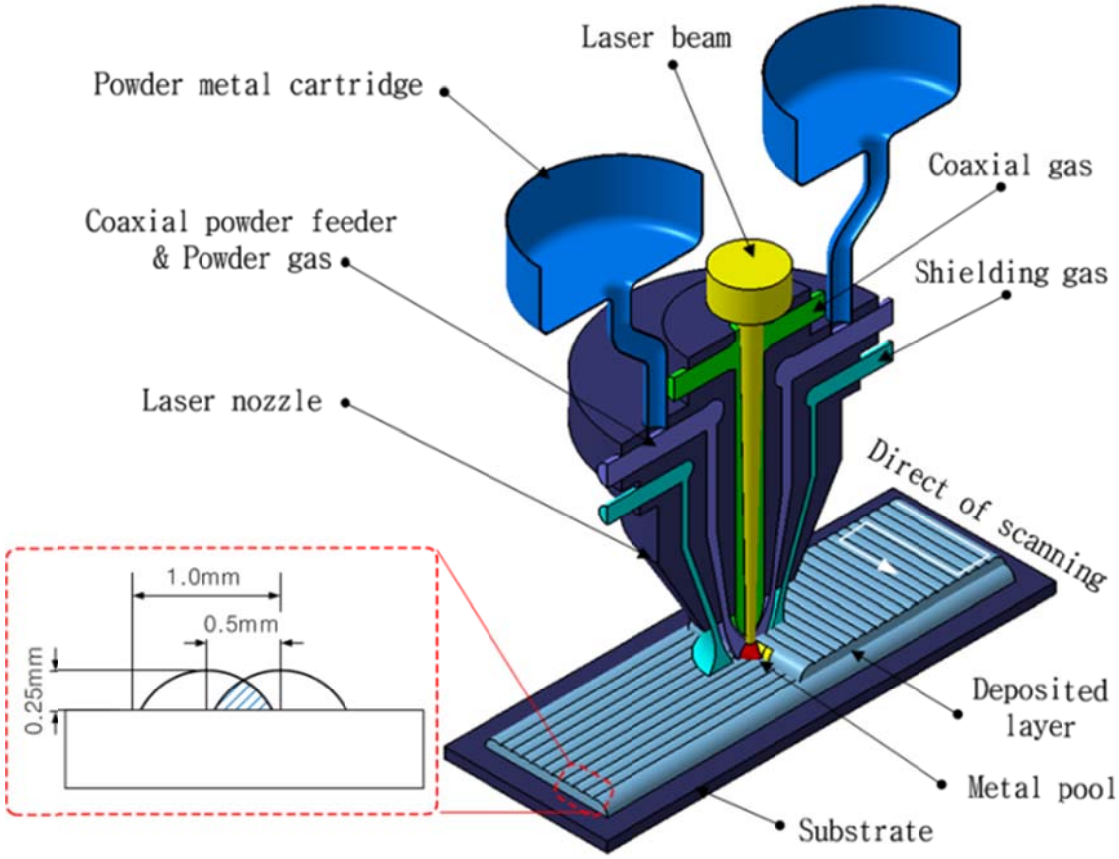

Fig. 2.1 Description of the laser melted metal deposition and DED system.

The powder feed gas supplies powder for the formation of molten pool on the substrate surface, while the coaxial gas prevents oxidation of the molten pool by injecting the protect gas around the laser beam. In order to prevent substrate oxidation due to heat from the laser, metal powder is continuously injected into the pool which is melted with inert argon (Ar). The metal powder is supplied in real time through the coaxial powder feeder to melt state and rapidly solidified to form a metal layer having a dense structure.

2.2 Other additive manufacturing method

2.2.1. PBF (Powder Bed Fusion)

In the powder bed fusion process, a thin layer of metal powder is deposited on the substrate and the metal powder is melted using an energy source (laser or electron beam) [19].

After the completion of a layer, a layer of new metal powder will be placed on the basis of last layer. And the energy source repeats the previous trip. So repeatedly, the 3D part will be manufactured on a metal powder bed as shown in Figure 2.2.

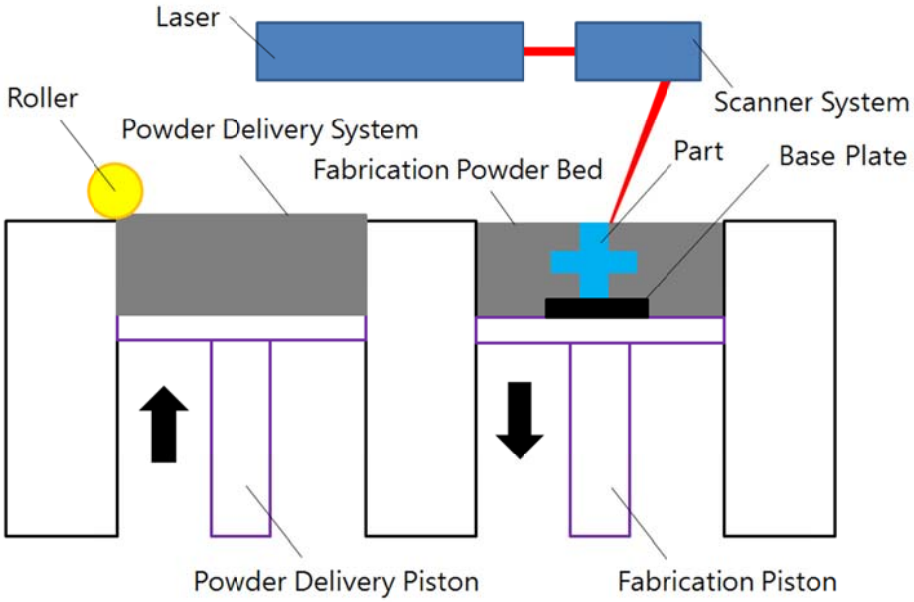

Fig. 2.2 The schematic diagram of the PBF (Powder Bed Fusion)

2.2.2. SLS, SLM, and other methods

Selective laser sintering (SLS) is an additive manufacturing (AM) technique that uses a laser as the power source to sinter powdered material (typically nylon/polyamide), aiming the laser automatically at points in space defined by a 3D model, binding the material together to create a solid structure. It is similar to direct metal laser sintering (DMLS); the two are instantiating of the same concept but differ in technical details. Selective laser melting (SLM) uses a comparable concept, but in SLM the material is fully melted rather than sintered, allowing different properties (crystal structure, porosity, and so on). SLS (as well as the other mentioned AM techniques) is a relatively new technology that so far has mainly been used for rapid prototyping and for low-volume production of component parts. Production roles are expanding as the commercialization of AM technology improves.

Selective laser melting (SLM) or direct metal laser sintering (DMLS) is a particularly rapid prototyping, 3D printing, or Additive Manufacturing (AM) technique designed to use a high power-density laser to melt and fuse metallic powders together. In many SLM is considered to be a subcategory of Selective Laser Sintering (SLS). The SLM process has the ability to fully melt the metal material into a solid 3D-dimensional part unlike SLS.

Also, there are some other 3D print methods like EBF (Electron-beam freeform fabrication), EBM (Electron-beam additive manufacturing) and SHS (Selective heat sintering) which used in different conditions of the materials.

In the field of manufacturing, many different kinds of 3D printing technologies have emerged. Different technologies have their own advantages and disadvantages. In this paper, the main method is DED technology and the PBF method will be the reference and comparison [20].

Chapter 3 Additive manufacturing powder metal materials

Metal powder refers to a group of metal particles having a size of less than 1 mm. Single metal powders, alloy powders, and certain refractory compound powders with metallic properties are the main raw materials for powder metallurgy. Metal powders are loose materials. The properties of metal powders are generally classified into chemical properties, physical properties, and process properties. Chemical properties refer to metal content and impurity content. The physical properties include the average particle size and particle size distribution of the powder, true density of the powder, the shape of the particles, and the microstructure. Process performance is a comprehensive property which mainly embodied in specimens after additive manufacturing.

For material selection, the mechanical properties of the bulk material are the basic criteria initially selected. However, the choice of materials depends on the certain purpose. For example, if the material to be printed has high strength, high-strength bulk materials will be of particular concern during the initial selection process. Similarly, the goal is to have a material with high strength and high wear resistance in this study. At the beginning, there are many bulk materials that meet the goals such as SKD-11 HWS SKD-51 and so on as shown in Table 3.1. The reason for choosing these types is that they have high hardness, high toughness, and high wear resistance. In the PBF method, the material metal is used as high-strength mold steel powder materials. But in the DED method, the high wear resistance steel is used such as HWS.

Table 3.1 Existing physical properties data of bulk materials

Items	SKD11 (D2)	HWS	SKH51 (M2)	K340	VANDA DIS	SKD61 (H-13)	HTCS-130
Density [kg/m^3]	7670			7680		4230	8060
Young Modulus[GPa]	207		190-210	206.1	225-234		210
Achievable hardness [HRc]	60-62	60-64	62	57-59 /60-62	62	314Hv	44 (50-65)
Charpy resilience [J]	25(77)	110	67		17.5	33	
Wear resistance	100	700					
Yield tensile strength [MPa]			350-550	2173		215	1225
Ultimate tensile strength [MPa]	2181	2715	650-880	2550		493	
Strain [%]	1.62	2.24		2.81			
Poisson's ratio	0.27-0.3		0.27-0.3				0.3
Compression strength [MPa]	3472	4306		2480/2670			
Fracture toughness [MPa.m$^{1/2}$]				17.2			
Strain under compression [%]	8.5	12.46					
Bending strength [MPa]	2951	4382					
Bending strength transversal [MPa]	1526	4315					
Isotropy of bending strength [%]	52%	98%					
Specific heat capacity [J/(g.K)]				0.49			0.47
Thermal conductivity [W/(m.K)]				17.8			58
Thermal expansion coefficient(100℃) [10^{-6}m/(m.K)]	10.4			11.0			12.2

From the materials of the physical properties data, the HWS shows a better overall performance. The hardness of it is 60.64 and the Charpy resilience is 110J. Best of all, it shows a high wear resistance. So, the powder material of HWS is selected as the preliminary analysis.

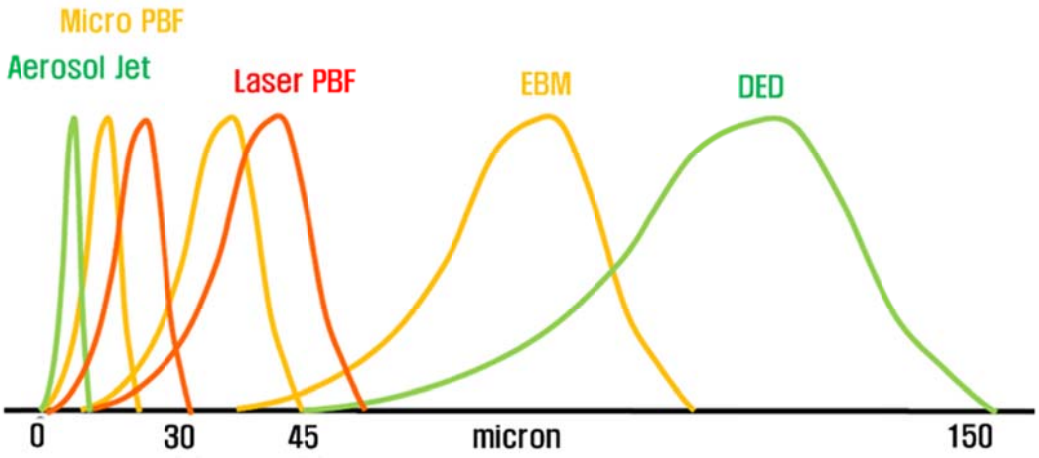

Fig. 3.1 Powder particle size criterion according to 3DP method

The properties of the powder metal and the properties of the bulk material are certainly not the same. The comparison of specific parameters must be completed after the additive manufacturing. The production of metal powder becomes more important. For particle size, the best range for DED technology is 50μm-150μm as shown in Figure 3.1 [21].

In order to further analyze HWS powder metal materials, SEM analysis, chemical compositions, particle analysis will be performed.

3.1 SEM image of HWS powder

A scanning electron microscope (SEM) is a type of electron microscope that produces images of a sample by scanning the surface with a focused beam of electrons. By scanning electron microscopy, we can observe the surface morphology of the material as shown in Figure 3.2.

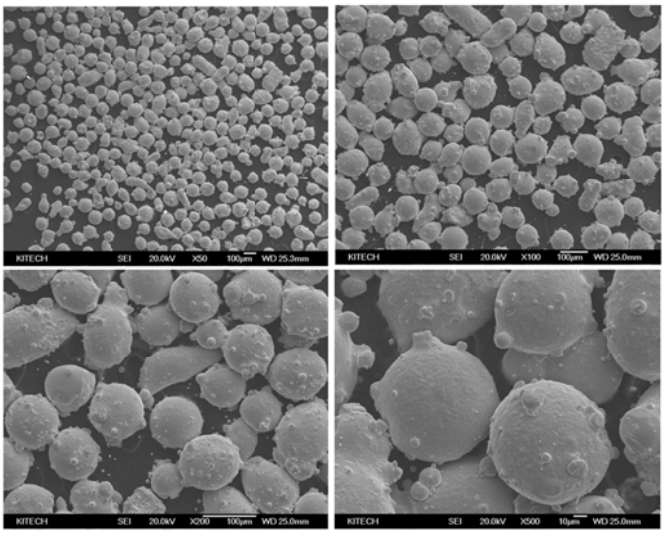

Fig. 3.2 The SEM image of HWS powder material

In the 200-fold image, many small satellite particles appear in the blank space. In the fourth 500-fold image, it can be seen that satellite spherical powders adhere to the particles. And the number is large, causing the roundness of the particles to decrease. The powder particles of HWS have poor quality compared to the other two powder metals suitable for DED technology as shown in Figure 3.3.

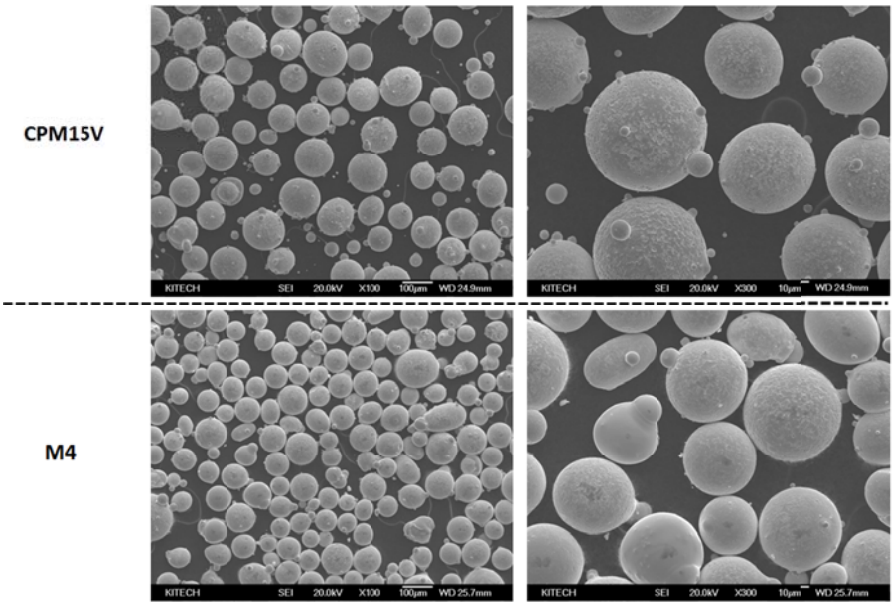

Fig. 3.3 The SEM image of CPM15V and M4 powder material

3.2 Chemical compositions of HWS powder material

Table 3.2 Chemical compositions of HWS powder and compare items

Materials used	Element (wt %)										
	C	Si	Mn	P	S	Ni	Cr	Mo	Cu	V	W
HWS powder	1.08	1.38	0.34	-	-	-	7.80	1.86	-	2.66	1.73
SKD11 OR D2 (substrate)	1.56	0.24	0.25	0.025	0.001	0.175	11.31	0.83	0.14	0.25	-
AISI M4 powder	1.33	0.33	0.26	0.03	0.03	0.3	4.25	4.88	0.25	4.12	5.88
CPM15V powder	3.55	0.91	0.40	0.023	0.017	0.17	5.24	1.26	0.11	14.84	0.09

The HWS powder contains alloying elements such as chromium (Cr), molybdenum (Mo), tungsten (W), vanadium (V), manganese (Mn), silicon (Si). It is a high carbon alloy tool steel as shown in Table 3.2.

3.3 Particle analysis

An imaging particle size distribution test was developed by the image particle analysis system and multi-functional particle analysis system such as particle type appearance analysis. It is a product that combines traditional microscopic measurement methods with modern image processing techniques. Its basic workflow is to capture the image of the microscope through a dedicated digital camera. The particle image is transmitted to the computer with USB data transfer. Processing and analysis of images through specialized particle image analysis software. The analysis results are output through the monitor. The system has features such as intuitiveness, image, accuracy, wide test range, automatic identification, automatic statistics, and automatic calibration. Not only it can be used to observe the particle morphology, but also can obtain the particle size distribution, the average aspect ratio, and the

aspect ratio distribution. It added a new granularity test method for scientific research and production. It includes particle size, particle shape as well as distributions of statistical population measurements.

Distribution of circularity and diameter is shown in Figure 3.4. The abscissa in the figure shows the diameter of the particles. The ordinate in the figure shows the circularity of the particles. If the circularity of the particle is close to a perfect circle, the value is close to 1. After the pattern is obtained, it is found that the satellite particles are present in the powder metal material. Satellite particle size is mainly distributed in about 10μm. Therefore, we proposed a deionization process in order to make sure that the particle size is distributed in 50μm-150μm. The shape analysis of 5000 samples of HWS showed that the powder was close to spherical.

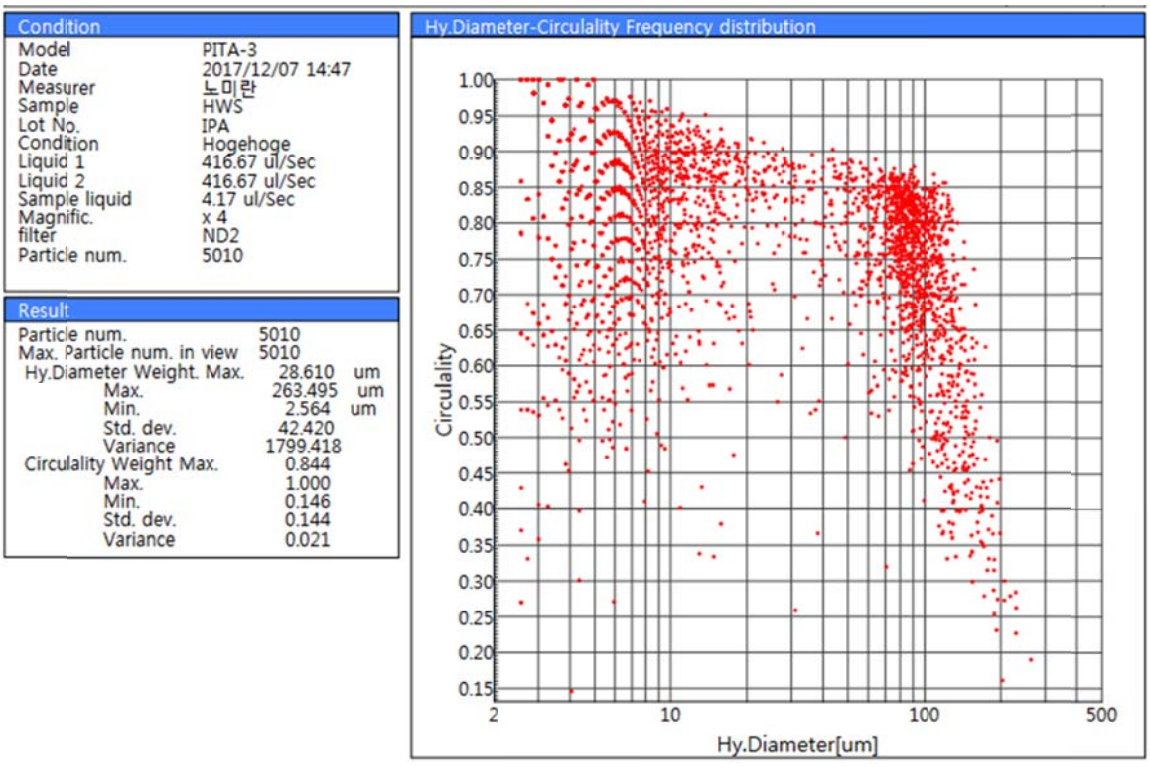

Fig. 3.4 The circularity and the diameter

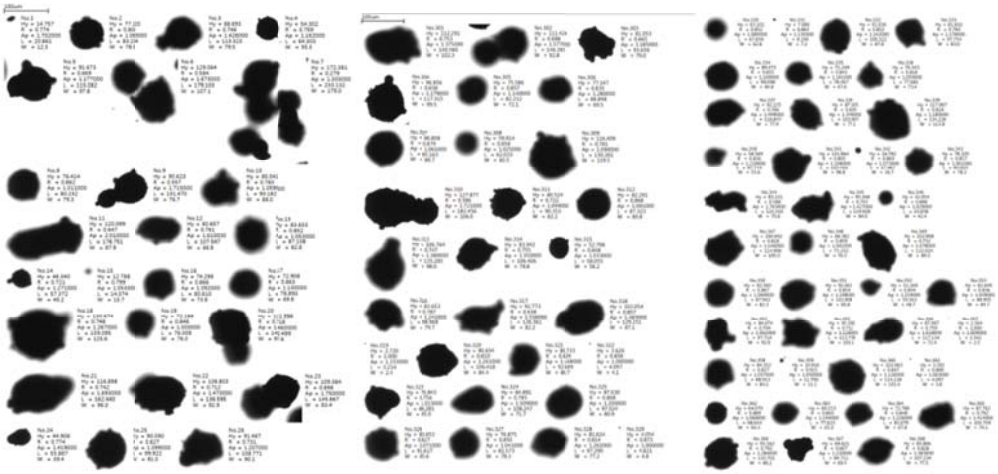

Fig. 3.5 The shape analysis image

The shape analysis image shows the circularity of the particles as shown in Figure 3.5. From this image, you can roughly see the shape of the particles. And, the radius, length, and width of the particles are also shown in the detailed results. The particle size analysis is shown in Figure 3.6. Among them, the abscissa is the diameter of the particle. The frequency of particle appearance and accumulate are shown in the ordinate. There are some fine powders and medium to large powders. On average 80-160μm powder is the mostly distributed (DED applicable). The proportion of satellite particles and large particles is also small.

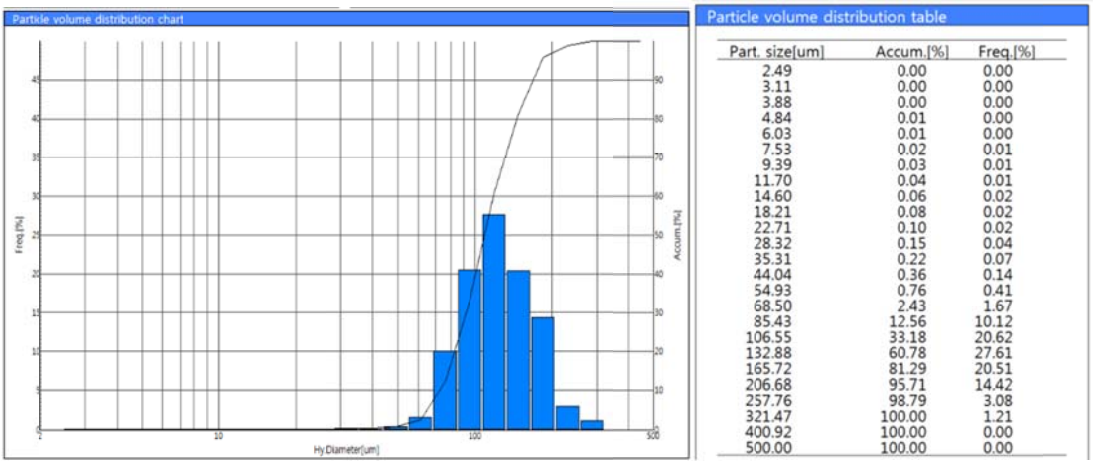

Part. size[um]	Accum.[%]	Freq.[%]
2.49	0.00	0.00
3.11	0.00	0.00
3.88	0.00	0.00
4.84	0.01	0.00
6.03	0.01	0.00
7.53	0.02	0.01
9.39	0.03	0.01
11.70	0.04	0.01
14.60	0.06	0.02
18.21	0.08	0.02
22.71	0.10	0.02
28.32	0.15	0.04
35.31	0.22	0.07
44.04	0.36	0.14
54.93	0.76	0.41
68.50	2.43	1.67
85.43	12.56	10.12
106.55	33.18	20.62
132.88	60.78	27.61
165.72	81.29	20.51
206.68	95.71	14.42
257.76	98.79	3.08
321.47	100.00	1.21
400.92	100.00	0.00
500.00	100.00	0.00

Fig. 3.6 The particle size analysis

Chapter 4 The fabrication of the specimens

4.1 The equipment and parameters

DED equipment is developing from DMT (Direct Metal Tooling) MX3 metal printing equipment developed by Insstek (Korea) Co., Ltd. The schematic is shown in Figure 4.1 and Figure 4.2. The equipment is built up by a laser heat source, numerical control system, five axis NC machine tool, powder feeding system and corresponding software system. For this equipment, it uses a TRUMP TLF 4000 with a maximum output of 2 kW, the beam diameter of 0.8 to 1.0 mm and a laser of 4 kW CO2. Numerical control system includes industrial operation computer, tilting and rotating device. The five axis NC machine tool includes X, Y, Z, tilt and rotation. A powder feeding system is consisted of three hoppers and a coaxial powder nozzle. Software system is MX-CAM software.

The track moves back and forth in a fixed direction. The beam spot diameter was 1.0 mm with a top-hat intensity distribution. Overlapping tracks have a pitch of 0.5mm. Argon is used as a shielding gas. The machining head with concentric powder is integrated with the optical system to supply powder coaxially with the laser beam to the substrate surface which is 9 mm away from the nozzle tip.

The powder feed gas supplies powder for the formation of molten pool on the substrate surface, while the coaxial gas prevents oxidation of the molten pool by injecting the protect gas around the laser beam. In order to prevent substrate oxidation due to heat from the laser, metal powder is continuously injected into the pool which is melted with inert argon (Ar). The metal powder supplied in real time through the coaxial powder feeder to melt state and rapidly solidified to form a metal layer having a dense structure.

Fig. 4.1 DED equipment, (DMT 3D metal printers MX3, Insstek Co., Ltd.)

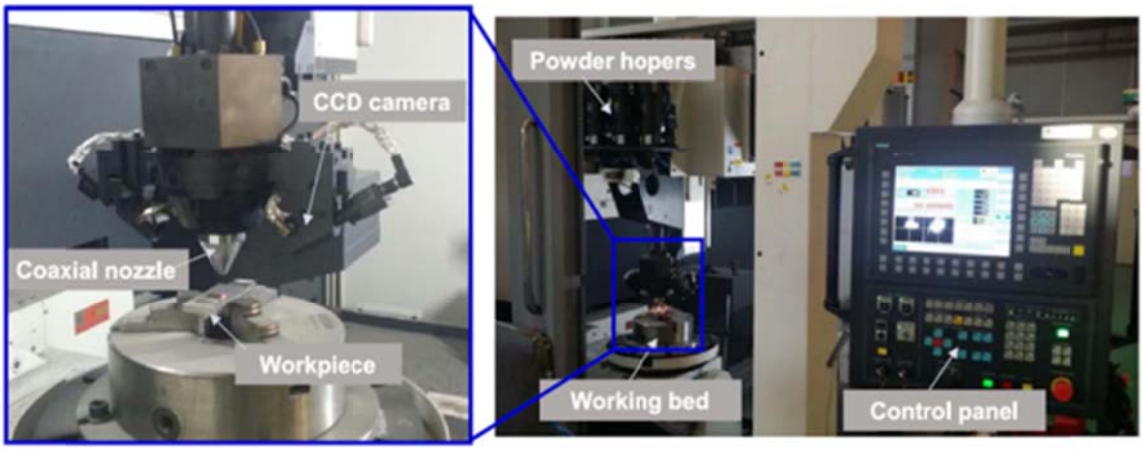

Fig. 4.2 The conditions of DED machine

The main parameters of the DED process include laser power powder feed rate, track scan interval and laser scanning speed. Potentially, different combinations of these parameters affect the mechanical properties and metallurgical properties such as roughness, hardness and microstructure of specimens. So, the mechanical properties and metallurgical properties of the resulting additive manufacturing part are subject to process variable effects. It is necessary to grasp the influence on the additive manufacturing characteristics through the combination of the process conditions which depend on the selected powder material. Because it is the process of obtaining optimum process conditions for manufacturing high-quality parts by DED technology.

Table 4.1 Parameters for DED processing

Laser power (W)	800
Slicing layer height (mm)	0.25
Overlap spacing(mm)	0.5
Powder feeding rate (g/mm)	5
Substrate traverse speed (mm/min)	850
Powder gas (ℓ/min)	2.5
Coaxial gas (ℓ/min)	8.0

Particularly, in this study, the most important factor in the semi-additive manufacturing part (partial layer) of the heterogeneous material using the DED method is the completed bonding between the substrate material and the AM material. It is important to find a key point that can be satisfied according to the applied material. The process of optimizing the process conditions between heterogeneous materials requires a lot of trial and error. In this study, the AM process conditions between the substrate material D2 and the HWS powder material are shown in Table 4.1.

4.2 The specimens

The use of DED technology for additive manufacturing requires post-processing of the specimen after printing. This is due to the fact that the surface quality after additive manufacturing is very rough, and that the additive manufacturing portion is printed on the substrate. The portion to which the HWS powder material is added is one layer. If full additive manufacturing specimens are required, a certain thickness must be printed on the substrate and then cut. However, in order to ensure the purity of full additive part, it is necessary to pay attention to leaving enough margins. In this study, the compression test specimens are fabricated by full-additive manufacturing. But the impact test specimens and wear test specimens are manufactured by semi-additive manufacturing. Compared to the PBF method, partial additive manufacturing is difficult to achieve. So, the semi-additive manufacturing specimens and punches will not be fabricated.

In the manufacturing process, the laser power is 800W. The slicing layer height is 0.25mm. Overlap spacing is 0.5mm. The powder feeding rate is 5g/mm. Substrate traverse speed is 850mm/min. The powder gas is 2.5l/min. And the coaxial gas is 8.0l/min. In the printing process, the single-layer track has a width of about 1 mm and a height of about 0.25 mm. And track trajectories are printed in a zigzag line by line. After the single layer is over, the next layer is increased layer by layer on a single layer basis. The machining allowance was within 1mm according to the shape characteristics of each test specimen.

The compression specimen is fabricated by full additive manufacturing which is different from other specimens. The sample is a cylinder whose diameter is 5mm and the height of sample is 5mm according to ASTM E9-89a [22]. The compression test piece is printed on the substrate and then cut to form a cylinder which is fabricated by HWS powder material. As the image shows, the Figure 4.3(a) is the dimensions. The Figure 4.3(b) shows the 3D stereogram. Figure 4.3(c) shows the D2 substrate and AM HWS section. Figure 4.3(d) shows the compression test specimens.

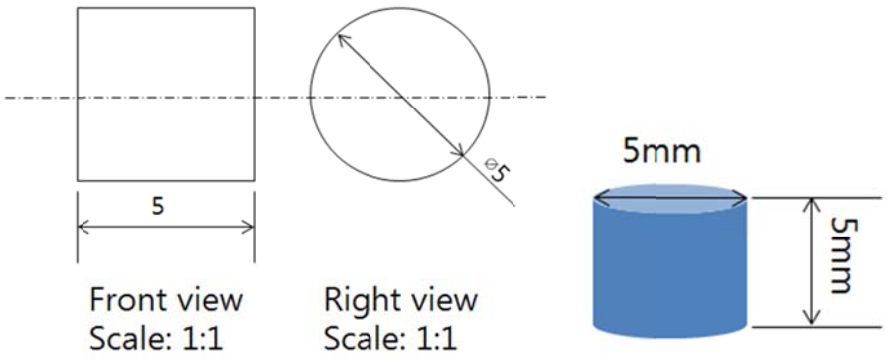

(a) (b)

(c)

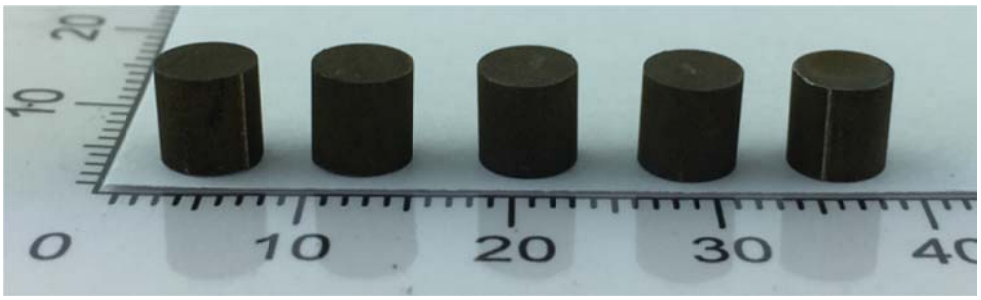

(d)

Fig. 4.3 (a) the standard dimensions of compression test specimens (unit: mm) (b) the 3D stereogram (c) after additive manufacturing (d) the compression test specimens.

Impact specimen is according to ASTM E23 with U-Notch [23]. The thickness of the test piece is 10 mm, in which the additive manufacturing portion and the substrate portion each takes half. The thickness of AM part is 5.75mm before cutting in order to leave enough margins. The D2 substrate size is 60mm×100mm×10mm. According to the standard, U-shaped notches with a depth of 2 mm are machined after the rectangular parallelepiped test specimen completed. The depth of the notch is 2mm, but it includes a semicircular arc with a radius of 1mm. The U-Notch opens in the additive manufacturing section. As shown in Figure 4.4, the blue part is AM layer and the gray layer is the substrate. As the image shows, the Figure 4.4(a) is the dimensions. The Figure 4.4(b) shows the 3D stereogram. Figure 4.4(c) shows the D2 substrate and AM HWS section. Figure 4.4(d) shows the impact test specimens.

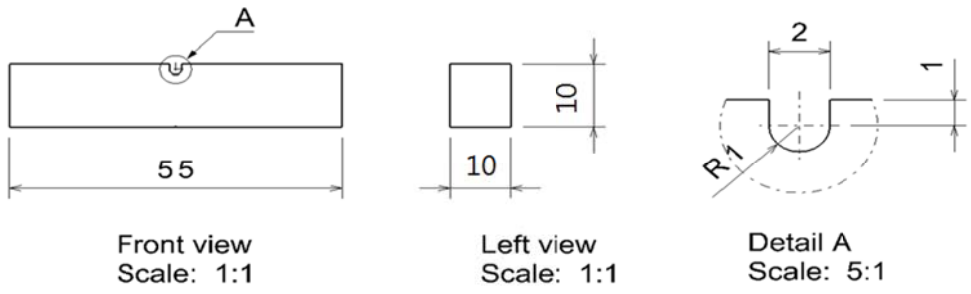

(a)

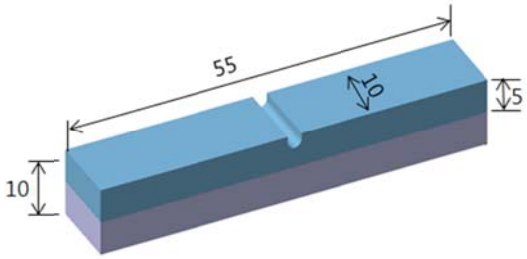

(b)

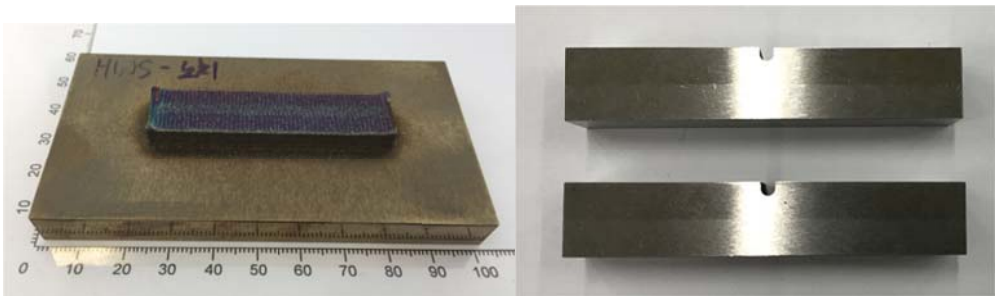

(c) (d)

Fig. 4.4 (a) the standard dimensions of impact test specimens (unit: mm) (b) the 3D stereogram (c) after additive manufacturing (d) the impact test specimens.

Wear specimen has only 1mm thick additive manufacturing layer on the top surface. The balls were set to rotate at the top surface of the specimen for 10 minutes using a ball-on-disk abrasion tester (R & B Inc.) under conditions of a load of 147.1N (15kgf) and a ball speed of 10.49 rad/sec. After the test, the weight loss of the test piece is exactly the amount of the HWS additive manufacturing after wear test. As the image shows, the Figure 4.5(a) is the dimensions. The Figure 4.5(b) shows the 3D stereogram. Figure 4.5(c) shows the D2 substrate and AM HWS section. Figure 4.5(d) shows the wear test specimens.

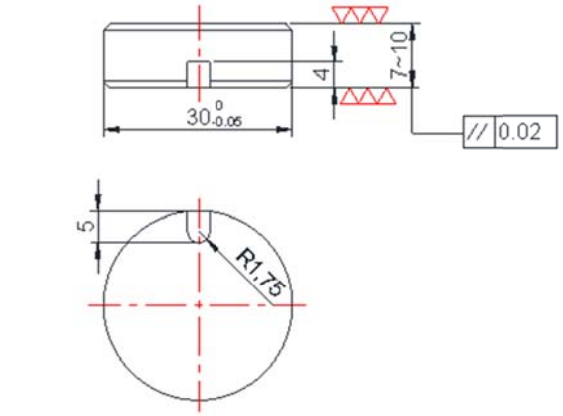

(a)

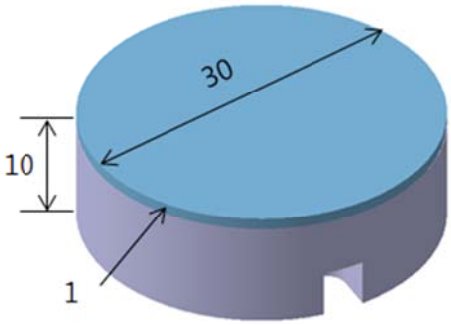

(b)

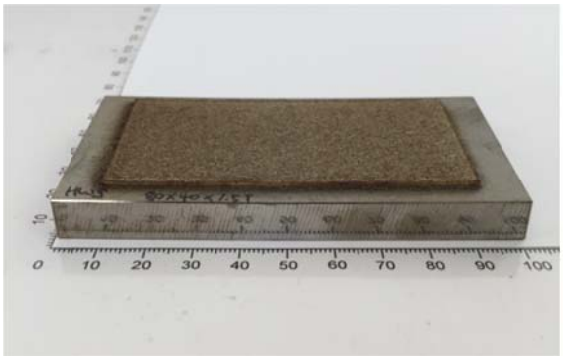

(c)

(d)

Fig. 4.5 (a) the standard dimensions of wear test specimens (b) the 3D stereogram (c) after additive manufacturing (d) the wear test specimens.

Chapter 5 Experiment setup and results

5.1 Hardness test

Hardness test was performed using HR-521 Rockwell hardness equipment from Akashi, Japan, shown in Figure 5.1. The hardness area was measured in the vertical direction, and a load of 150 kg was applied to each indentation for 15 seconds according to ASTM Standard Test Method E384 [24].

In Rockwell hardness test, the test force (initial test force F0 and total test force F0+F1) is applied to the surface of the test material twice in succession with a standard indenter, and the indenter is pressed into the surface of the sample under the test force. After the total test force is maintained for a certain period of time, the main test force F1 is removed. The indentation depth is measured with the initial test force F0 retained. The hardness is characterized by the difference between the indentation depth under the total test force and the indentation depth under the initial test force (residual indentation depth). The hardness value was obtained by calculating the area of the indentations made on the specimen using a penetrator. For different test pieces, we select more than three points on the same surface for measurement. Wear test specimens have one surface fabricated by AM HWS powder material. The number of selected surfaces for impact tests is relatively large, especially for the surfaces on both sides of U-shaped ports. Compression test specimens are not suitable for measuring hardness. Because the hardness test is after the original test, the compression test will destroy the quality of the surface.

Fig. 5.1 Hardness test equipment and mounting condition of hardness test specimen
(Hardness tester: HR-521 Rockwell hardness tester from Akashi, Japan)

5.2 Wear test

From the material point of view, the wear test is to evaluate the wear properties of the material to determine that the material is suitable for a particular wear application. Compared with other tests, wear tests are more affected by factors such as load, speed, temperature, surrounding media, surface roughness, lubrication, and coupling materials. Test conditions should be consistent with actual conditions as much as possible to ensure the reliability of test results. According to the movement, it can be divided into two types of sliding and rolling. According to different media it can be divided into 3 categories of dry friction, lubrication and abrasive. According to the specimen contact form, it can be divided into 5 categories: plane and plane; plane and cylinder; cylinder and cylinder; plane and ball. The wear tester is also divided into two types of unidirectional motion and reciprocating motion according to the direction of relative motion.

In wear test, we used a ball-on-disk abrasion tester (R & amp; B Inc.), shown in Figure 5.2. The ball was set to rotate at the top surface of the specimen for 10 minutes under conditions of a load of 147.1 N (15 kgf). The speed of it is 10.49 rad/sec. During this process, the ball rotates on the surface. Different scratches will appear on the surface of the specimen. In order to measure the reduction of the test piece material in wear, we need to measure the quality of the test piece before testing. After the end, it is necessary to measure the quality of the test piece again. Subtracting the two is the wear weight loss. And the coefficient of friction is calculated by the coefficient of friction = (load x distance) / (worn volume). Weight losses, width of wear track and friction coefficient were measured to evaluate the abrasion resistance of each specimen. In the case of AM specimens, the wear effectiveness is low and it is difficult to measure the wear amount by the weight measurement method. The width of the wear track is measured using a microscope tool. In particular, the wear test is performed before the hardness test.

Fig. 5.2 Wear test equipment and test condition of wear test specimen

5.3 Impact test

The Charpy impact test is performed to determine the notch sensitivity (toughness) of metallic materials. It has a U-shaped notch or V-shaped notch in preparation of a metal. In the Charpy impact tester, it is in the state of simply supported beam, and the pendulum lifted by the tester. The pendulum makes a shock and breaks the sample along the gap. When the specimen breaks, the difference in height at which the pendulum rebounds is used to calculate the absorption energy of the specimen.

The specimens are used to make specimens with 2 mm depth U-notches in accordance with ASTM E23 standard at room temperature. Impact energy, impact velocity and impact angle were set to 30J, 3.8m / s and 150 °, respectively. Hammer weight and panicle radius are 24.1kgf and 0.25m. . The equipment of impact test is Charpy Impactor from INSTRON. The shock absorbed energy was calculated from the set point and the shape of the fracture surface was investigated. The impact test conditions are shown in Figure 5.3.

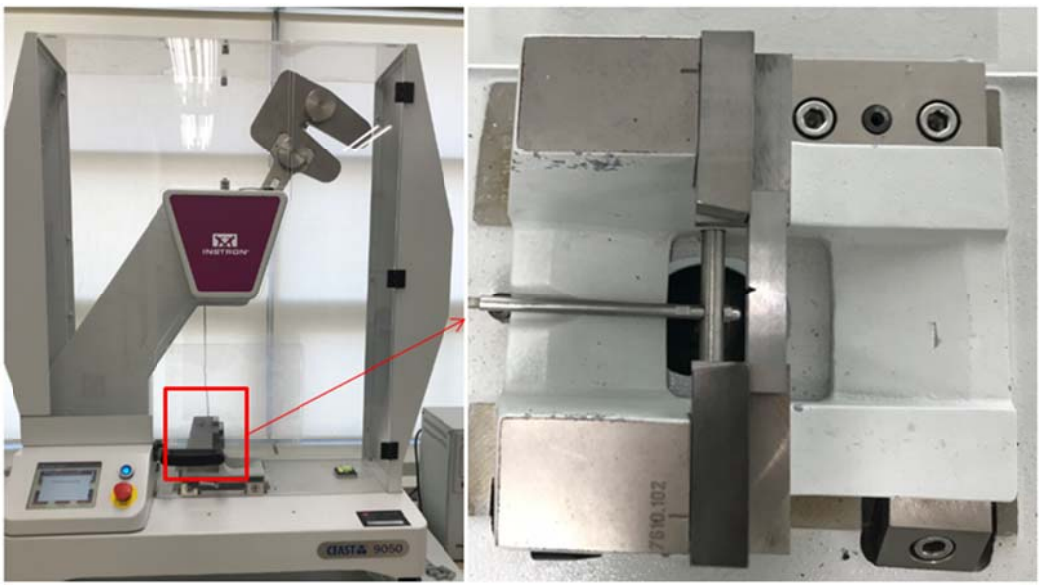

Fig. 5.3 Impact test equipment and mounting condition of impact test specimen

5.4 Compression test

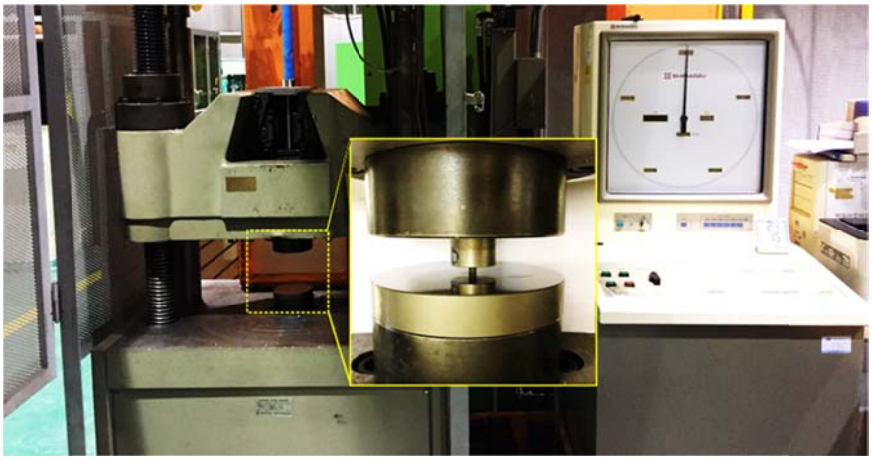

Fig. 5.4 Compression testing machine: Model 5582

The compression test is a method to determine the mechanical properties of a material under axial static pressure. It is one of the basic methods for testing the mechanical properties of materials. The maximum compressive load at failure of the specimen divided by the cross-sectional area of the specimen is called the compressive strength limit or the compressive strength. Compression curve can be made by a compression test. In this study, compression test equipment was Model 5582, Intron Corp. from USA as shown in Figure 5.4. And the compression test speed was 0.5mm / min.

5.5 Density test micro-CT

True density refers to the actual mass of a solid material per unit volume in an absolutely dense state. That is, the density after removal of internal pores or interparticle voids. The corresponding physical properties are apparent density and bulk density. The true density is the most basic physical parameter of the powder material, and it is also a parameter that must be used to determine the other physical properties such as particle distribution. The value of the true density depends on the chemical composition and purity of the material, and its value

directly affects the material quality, performance, application. It has great significance for its determination. In order for the additive material to have a dense structure, there should be no pores inside the material. This is possible when the laminated material and the powder material between the layer and the layer are completely melted at the same time to complete the metal and chemical bonding. Therefore, the structural density is one of the most important factors when evaluating additive manufacturing materials. Even if the mechanical properties are excellent, there are always some factors that may cause problems in the function.

In this study, the true density was measured by X-ray tomography as shown in Figure 5.5. The porosity of the specimen was measured using micro-CT (XT H 225, Nikon, Japan). The maximum operating voltage of the device is 225kV. The maximum operating power of the device is 225W. Focal spot size is from 3 μm (7 W) up to 225 μm (225 W). The camera has a pixel size of 127 μm and a 3-D image of the specimen is taken.

Fig. 5.5 Micro-CT Tomography: XT H 225 (Nikon, Japan)

5.6 Summary of experimental results

Through the wear test, the wear resistance of the material can be evaluated. Second, using the wear test results, the wear coefficient of each material could be calculated. So we can develop the appropriate heat treatment specifications to improve the mechanical properties of the material. The materials have more useful value, and can prolong the service life of the products and save the cost. Due to the narrow bandwidth of the wear portion, it is difficult to determine the amount of wear using the bandwidth. So in the results, only the amount of quality reduction is used to express. From the wear conditions of the surfaces, the trace of AM HWS after heat treatment is obviously light than the AM HWS before heat treatment. It means the wear resistance of the AM HWS becomes better after heat treatment. The results of the AM HWS after heat treatment is close to bulk HWS as shown in Table 5.1. But the AM HWS before shows the poor wear resistance. The wear resistance of AM HWS after heat treatment shows a better property. The results of the AM HWS after heat treatment is close to bulk HWS as shown in Figure 5.6. Under a unified standardized test method, the friction and wear performance indexes of various materials are measured.

Table 5.1 The results of wear test for AM HWS, bulk D2 and bulk HWS

Materials	Weight loss (mg)	
	Before heated	After heated
AM HWS	2.4	0.9
Bulk D2	-	3.75
Bulk HWS	-	0.54

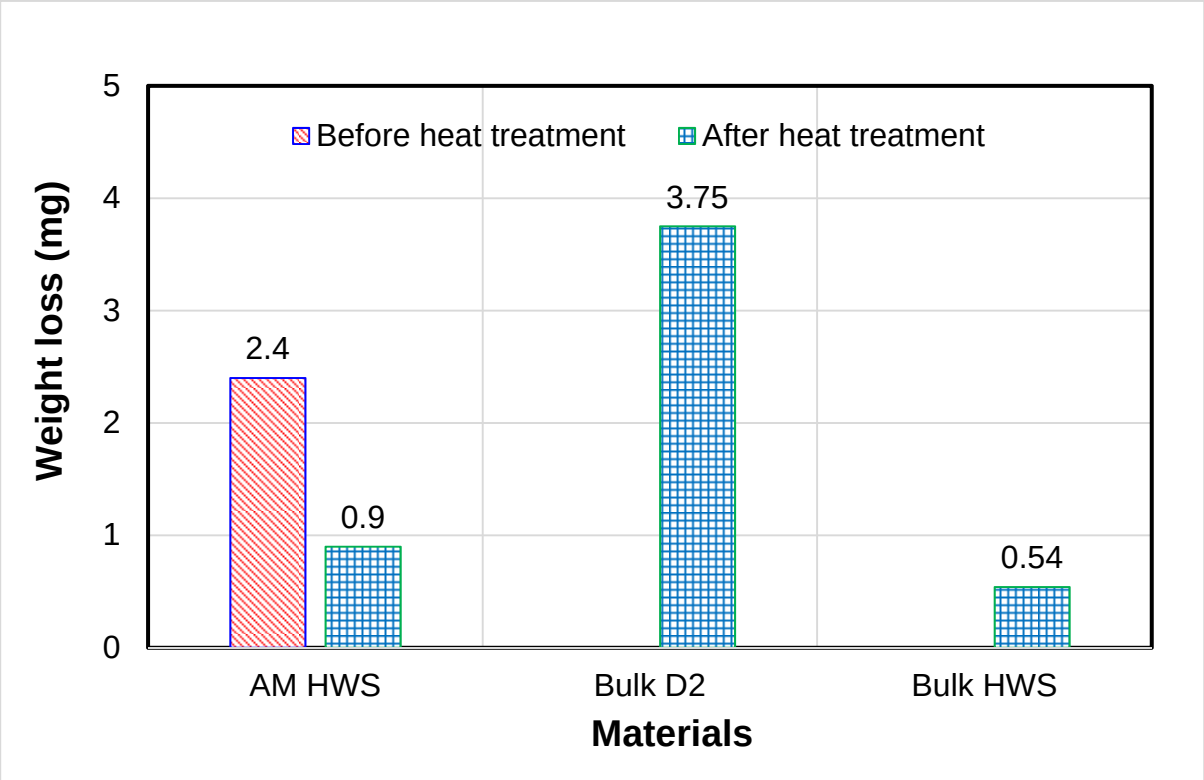

Fig. 5.6 The histogram of the result for wear test

In the results, only the HWS hardness value is relatively low, and the remaining results do not reflect a large difference as shown in Figure 5.7. Moreover, the hardness of HWS after heat treatment is 60.59HRc similar to the bulk HWS as shown in Table 5.2. Relatively speaking, the same kind of material is different according to the surface treatment and the hardness is proportional to the wear resistance. But not all high hardness materials will have good wear resistance. On the contrary, if it simply pursues the surface hardness, the hard materials will reduce the wear resistance of the friction surface. Additive manufacturing hardness values have been achieved the high hardness status like bulk materials and it shows a better wear resistance.

Table 5.2 The results of hardness test for AM HWS, bulk D2 and bulk HWS

Materials	Hardness (HRc)	
	Before heated	After heated
AM HWS	55.77	60.59
Bulk D2	-	61.0
Bulk HWS	-	62.0

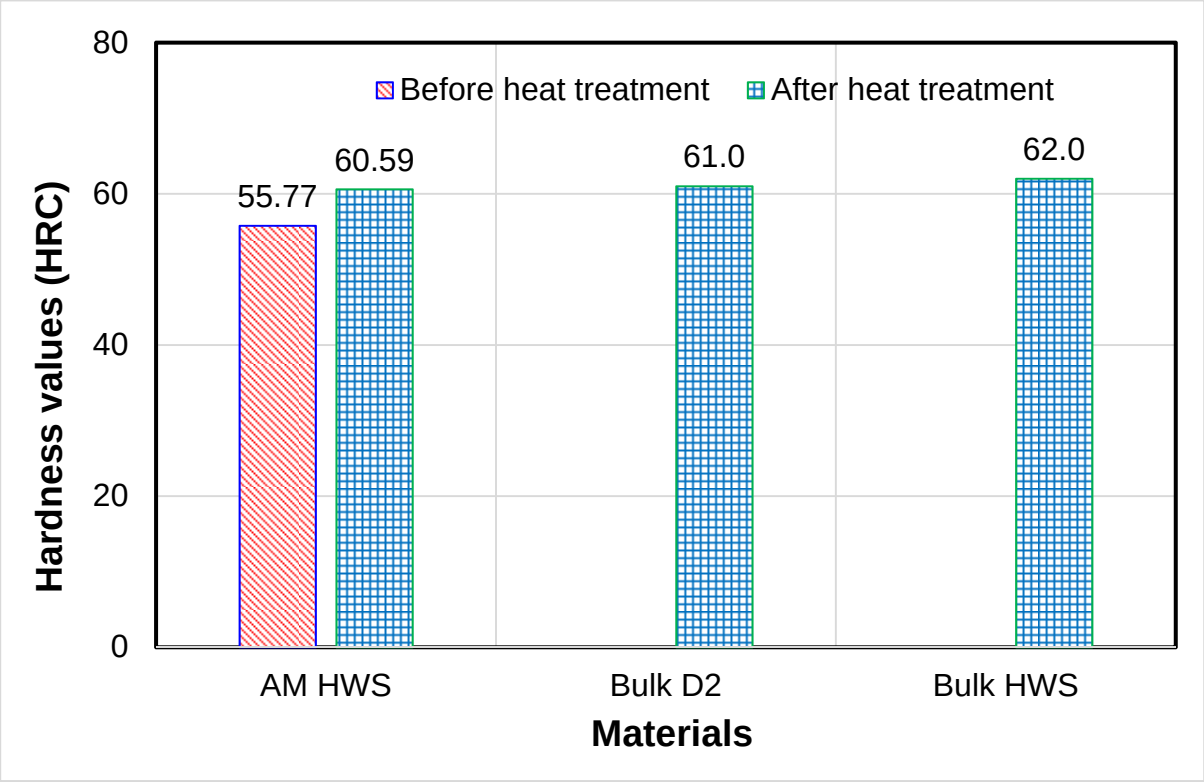

Fig. 5.7 The histogram of the result for hardness test

The purpose of the Charpy impact test is to test the notch sensitivity (toughness) of metallic materials. Toughness represents the ability of a material to absorb energy during plastic deformation and fracture. The better the toughness, the less likely it is to have a brittle fracture. In the results, the impact energy of the HWS powder AM specimens before and after the heat treatment was 5.0J and 5.64J as shown in Table 5.3. It was found that the target value is 22.5J, which is higher than the test value as shown in Figure 5.8. But it is 3.8 times better than D2, which is the comparative sample of this study. Because of the close to the bulk materials, it is necessary to tune the target value or the evaluation method

Table 5.3 The results of impact test for AM HWS, bulk D2 and bulk HWS

Materials	Absorbded Impact energy (J)	
	Before heated	After heated
AM HWS	5.00	5.64
Bulk D2	-	1.425
Bulk HWS	-	5.7

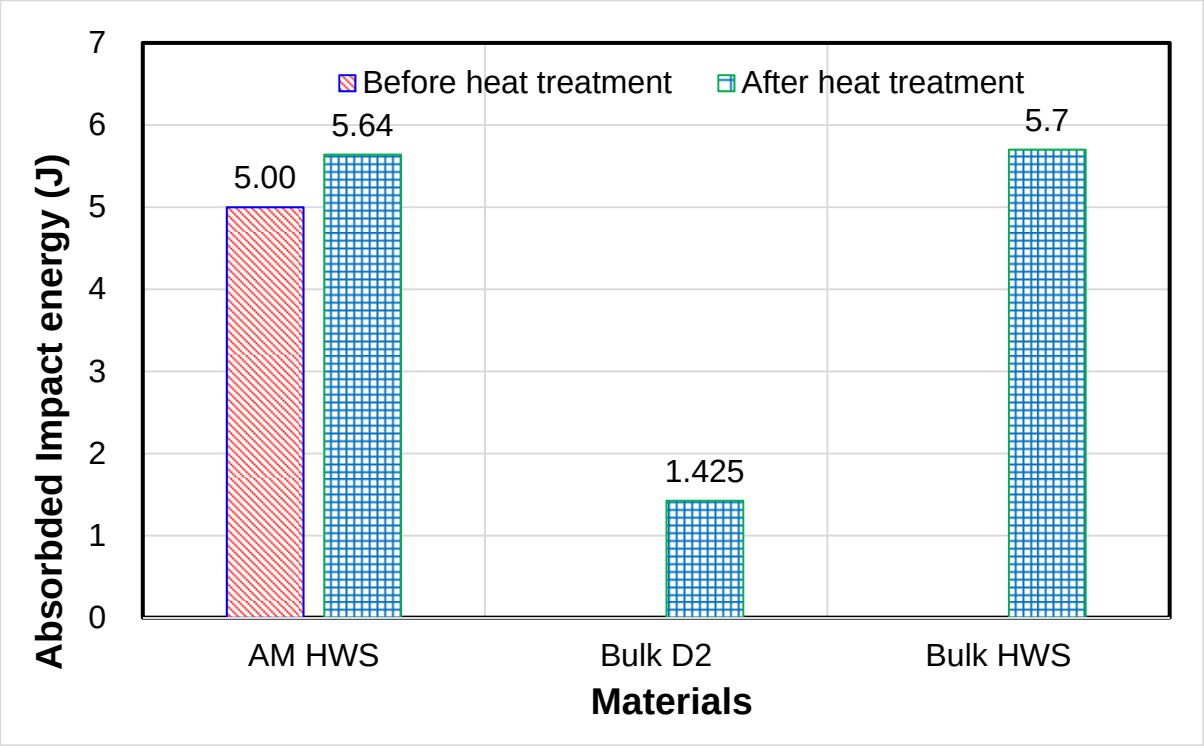

Fig. 5.8 The histogram of the result for impact test

The compression strength is one of the most important indexes for detecting punches. As shown in Table 5.4, the compression strength of AM HWS after heat treatment is 5044MPa which is higher than the other two value. The compression strength value becomes smaller with the heat treatment as shown in Figure 5.9. Compared to bulk materials, AM specimens show a good compression resistance obviously.

Table 5.4 The results of compression test for AM HWS, bulk D2 and bulk HWS

Materials	Compressive strength (MPa)	
	Before heated	After heated
AM HWS	5,513	5,044
Bulk D2		3,472
Bulk HWS		4,306

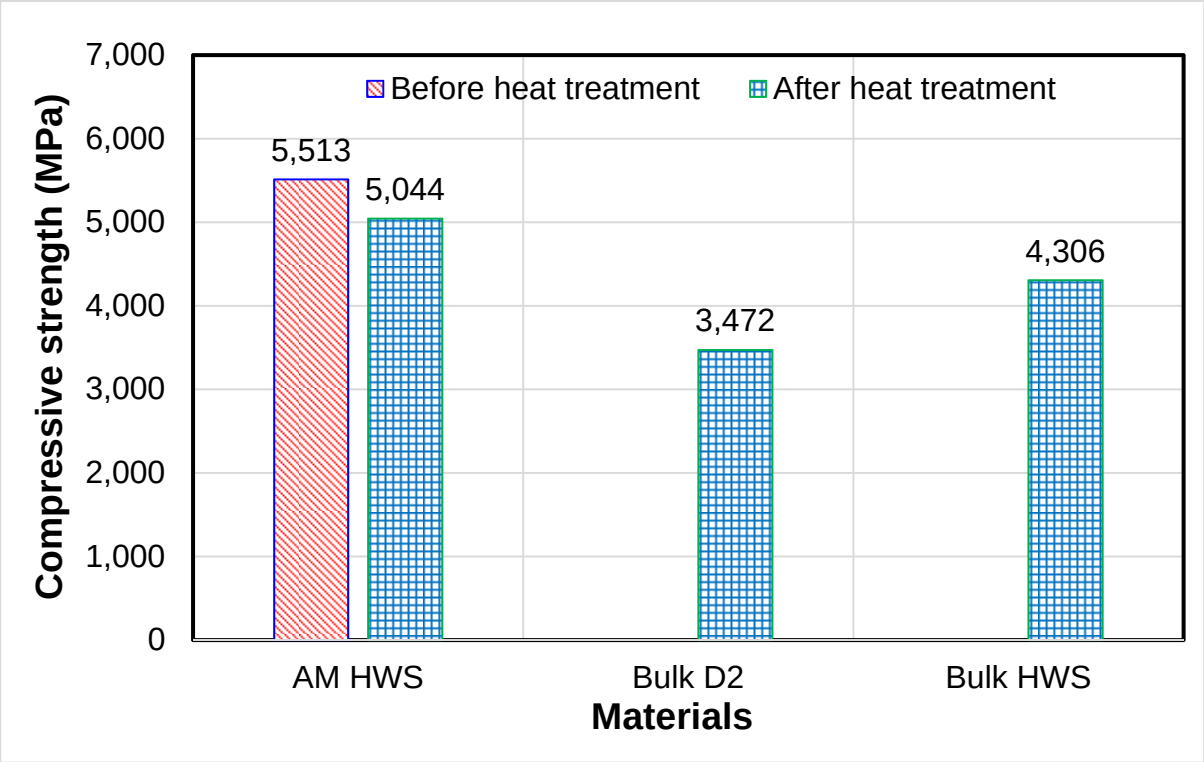

Fig. 5.9 The histogram of the result for compressive strength

The X-ray tomography results of the HWS powder AM HWS before heat treatment specimens showed a porosity of 0.01% and a true density of 99.99% as shown in Table 5.5. The X-ray tomography results of the HWS powder AM HWS after heat treatment specimens showed a porosity of 0.0% and a true density of 100.0% as shown in Figure 5.10. The hardness, toughness and true density of AM HWS specimens were improved by heat treatment. It has reached a considerable level with bulk materials.

Table 5.5 The results of true density for AM HWS, bulk D2 and bulk HWS

Materials	True density (%)	
	Before heated	After heated
AM HWS	99.99	100
Bulk D2	0	100
Bulk HWS	0	100

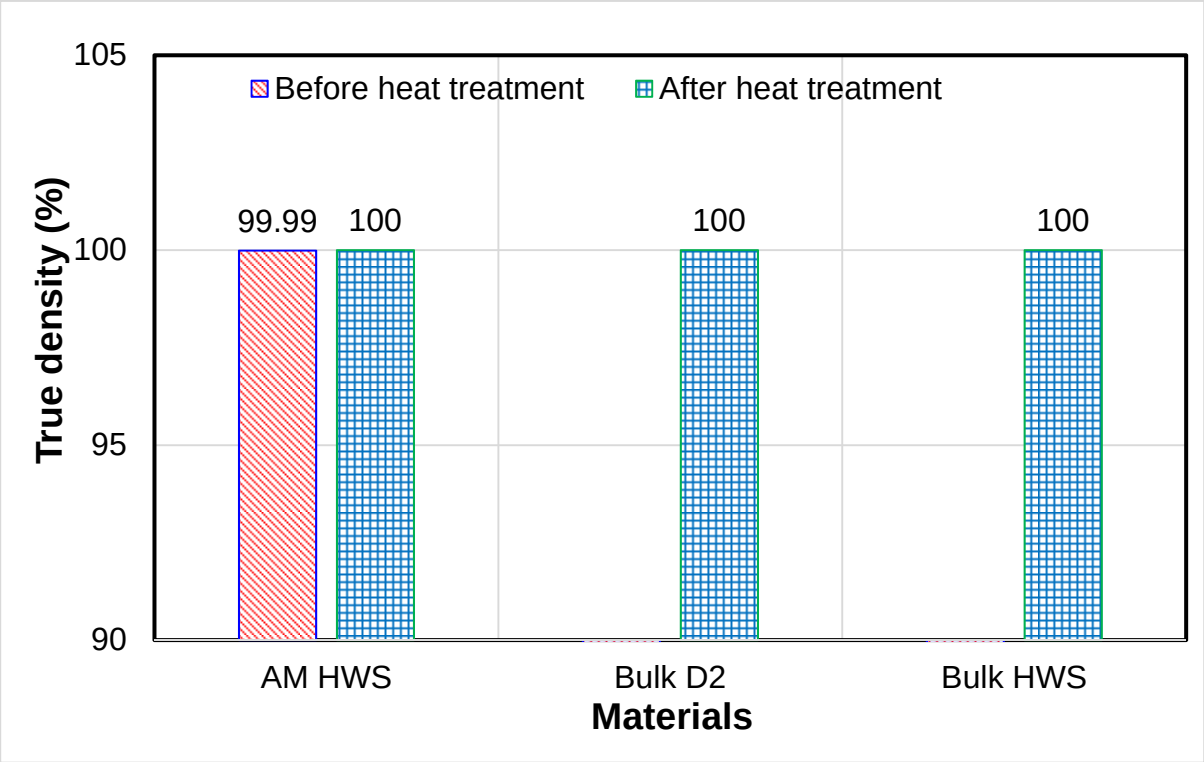

Fig. 5.10 The histogram of the result for true density

Chapter 6 The shape prediction of the semi-additive punch

We proposed a manufacturing method of semi-additive punching mold by using high strength powder material and 3DP technology to increase the strength of the part where strength is required. In order to select the shape range for the semi-additive punching mold which required for high-strength sheet material, the analytical simulation based on process analysis parameters is used to predict.

From the previously research, the average maximum stress acting on the punch in the piercing process of the high strength sheet material (CP1180) was 2,256MPa. The depth of the punch shape in which the stress is concentrated in the piercing process of the high strength sheet material (CP1180) is 1.21 mm. The height of the punch shape in which the stress is concentrated in the piercing process of the high strength sheet material (CP1180) is 2.625 mm. It was confirmed that the range (depth / height) of the semi-additive shape predicted in this study is within the range of 2 to 3 mm, which is a possible for the additive manufacturing of the high-strength metal mold powder material by 3D printing [15]. On this basis, we further analyzed the shape of the semi-additive punch.

6.1 Semi-Additive shape design

A simulation was performed to predict the punch strength required for the piercing process of the high strength sheet material CP1180 (1200MPa). From the simulation results, we predicted that the shape ranges for the depth (Ld) and height (Lh) of the punch shape affecting the punch strength due to shearing action are 1.21mm and 2.625mm. From the predicted punch shape range, several of shape types for the semi-additive were defined as showed in Figure 6.1.

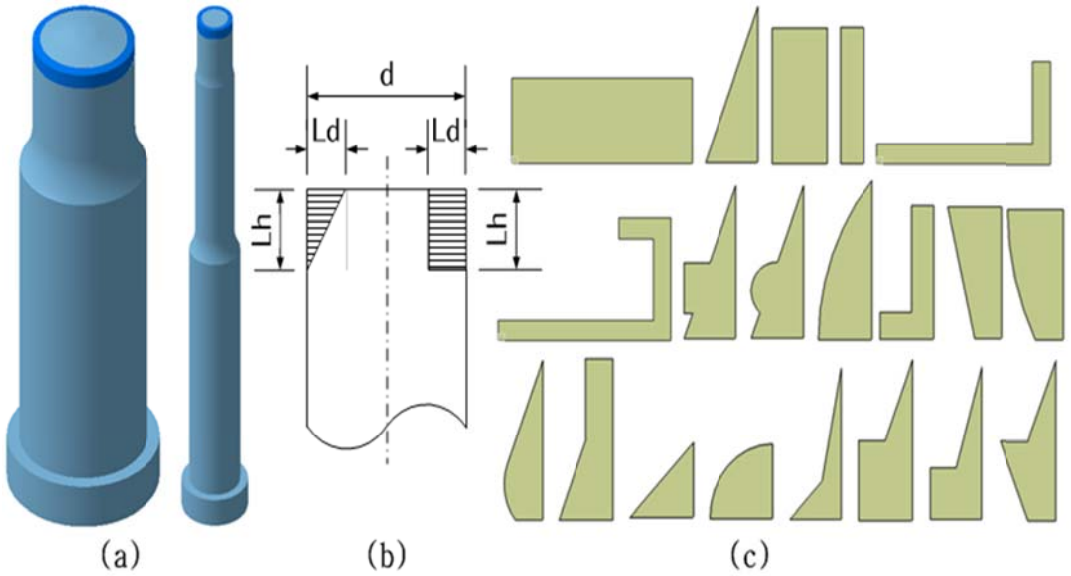

Fig. 6.1 (a) an example of a piercing punch body shape for a semi-additive, (b) a dimensional definition of a punch edge part shape for a semi-additive (c) variously types of semi-additive shapes.

First, an analysis was performed on the friction conditions at the boundary of semi-additive joints of different materials as a pre-simulation step for each semi-additive shape. This was performed to characterize the analysis software in advance for the optimization analysis of the semi-additive shape. In this interpretation, software interface boundary conditions are classified into Shear Friction (Sticking), Coulomb Friction (Sliding), Hybrid Friction, and Tau Friction. Here, the shear friction and coulomb friction conditions provide information on separation and slip at the bond interface boundary during the process. And tau friction conditions provide shear stress information at the surface. The hybrid friction condition means that the shear and coulomb conditions are applied at the same time. The phenomenon of separation and slipping can be observed at the joint interface boundary at the same time. In this analysis, it is defined as a technique for selecting boundary conditions, focusing on the shear material that adheres to the interface of different materials according to friction conditions, slip and peel change, and influences the fact of the damage value. Some of the analysis results are shown in Figure 6.2.

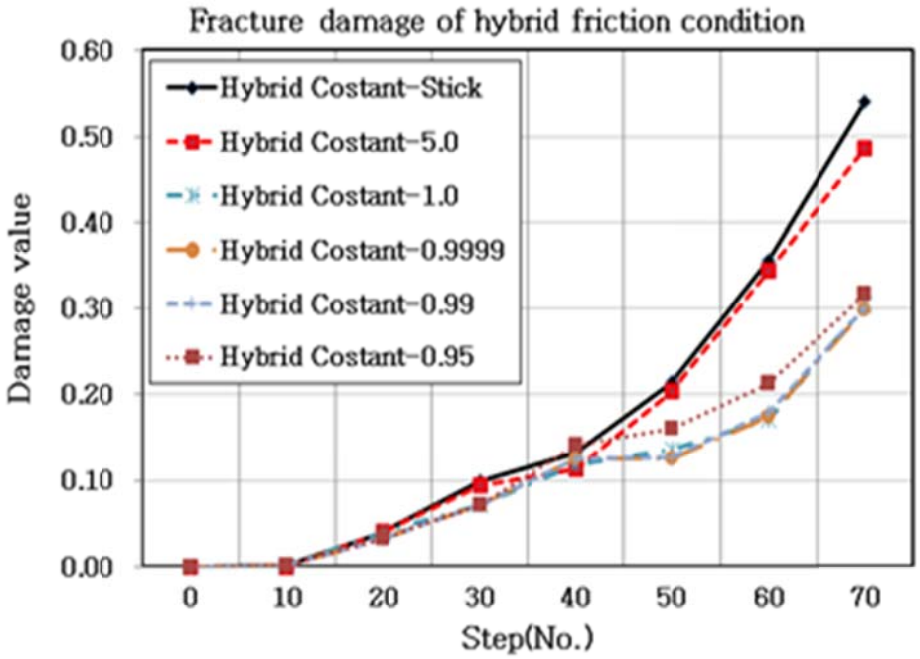

(a)

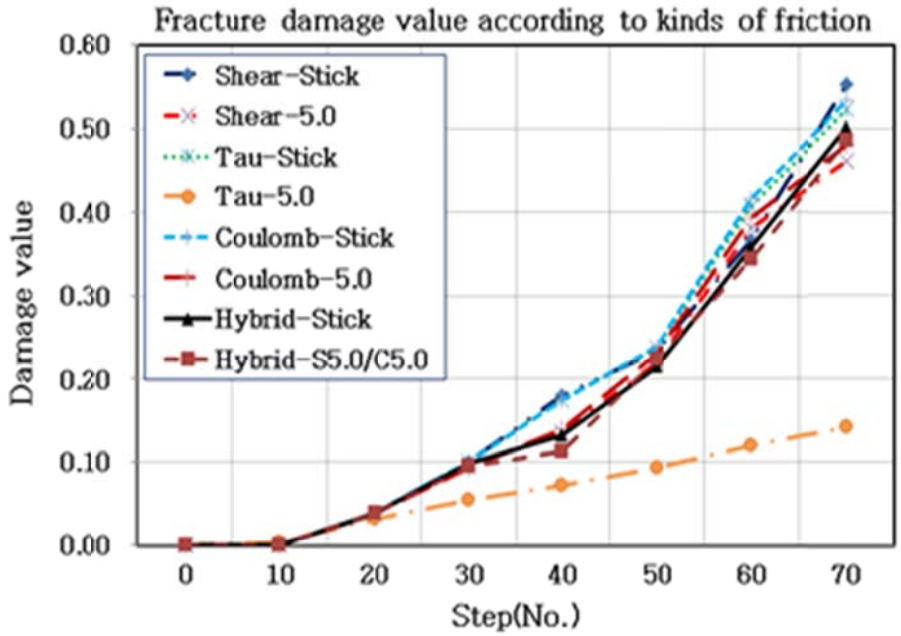

(b)

Fig. 6.2 (a) the comparison of the breakage damage values According to the size of the hybrid friction condition (b) the comparison of the breakage damage values According to the kinds of the friction condition.

For the results of this analysis, we cannot find a significant trend in software due to the variation of friction coefficient in shear friction, coulomb friction, and tau friction conditions.

So there is no explanation of this part. However, under the hybrid friction condition as shown in Figure 6.2 (a), the size of the damage value is small compared to other friction conditions. But it can be seen that tendency is significant according to the adjustment of the friction coefficient. It should be noted that the magnitude of the coefficient of friction presented here is conceptually different from the coefficient of friction applied as a condition for general molding operations. It is an exceptional value determined by software as a trial and error method for analysis. The fracture damage value according to the type of friction condition is shown in Figure 6.2 (b). It shows a similar tendency in other conditions except the tau condition. A friction coefficient at 1 and 5 shows significantly different trends under mixed friction conditions. The hybrid friction condition means that the boundary condition can be controlled at the joint surface according to the user's definition. Therefore, friction coefficient (shear and coulomb) of the hybrid type was selected as 5.0 for the friction condition of the process analysis to optimize the semi-additive shape for reinforcing the piercing punch function. Analytical studies and selected interfacial friction conditions were used as boundary conditions for the interface analysis of semi-additive shapes designed into various shapes.

6.2 Semi-additive simulation and results

The simulation of the selection of the shape of the half-plate is performed by studying the analysis conditions and software characteristics of the stamping process for the boundary friction conditions of the heterogeneous material interface. The simulation model is shown in Figure 6.3.

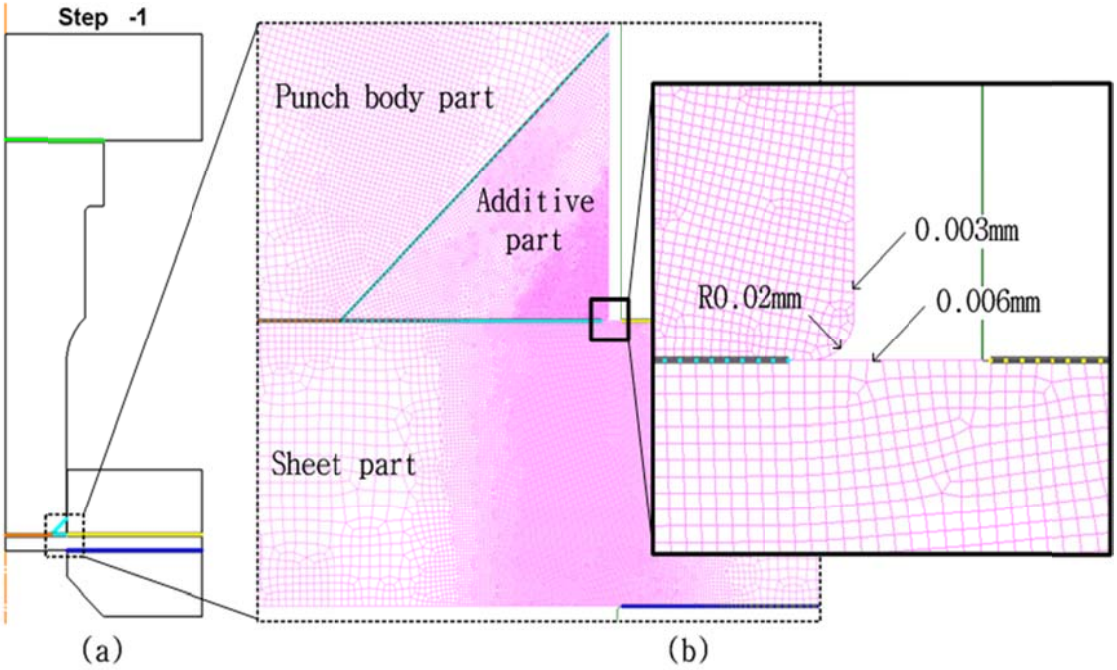

Fig. 6.3 Simulation analysis model: (a) contact boundary condition, (b) mesh element size

The analytical shape and the stress distribution of the simulation results for the optimal shape selection in the semi-additive shape are shown in Figure 6.4 and Figure 6.5. Figure 6.4 (a) shows an example of a plate type. It shows the most stable state among the simulated semi-additive shapes. Figure 6.4 (b) shows an example of an equilateral triangle type in which separation occurs at a joint interface boundary. Figure 6.4 (c) and (d) show the stress distribution and shear state of the sheet material. As shown in Figure 6.4 (a) and (b), the stress distribution for the case is observed from the most stable state of the semi-additive shape. The comparative stability is deteriorated due to separation at the bonding interface boundary. Figure 6.5 (a) shows a plate-type stress contour line which is the most stable state among the semi-additive shapes. It can be seen that stress contour progress smoothly from the sheet material to the punch body through the semi-additive range. However, it can be seen that the stress contour line in the semi-additive type has a triangular section with relatively poor stability due to separation at the joint interface in Figure 6.5 (b) and (c). And stress contours do not progress smoothly at the joint interface. In this semi-additive shape simulation analysis,

the maximum stress occurs at the beginning of shearing in the sheet material. It indicated that the punch stroke at the start of shearing on the sheet material.

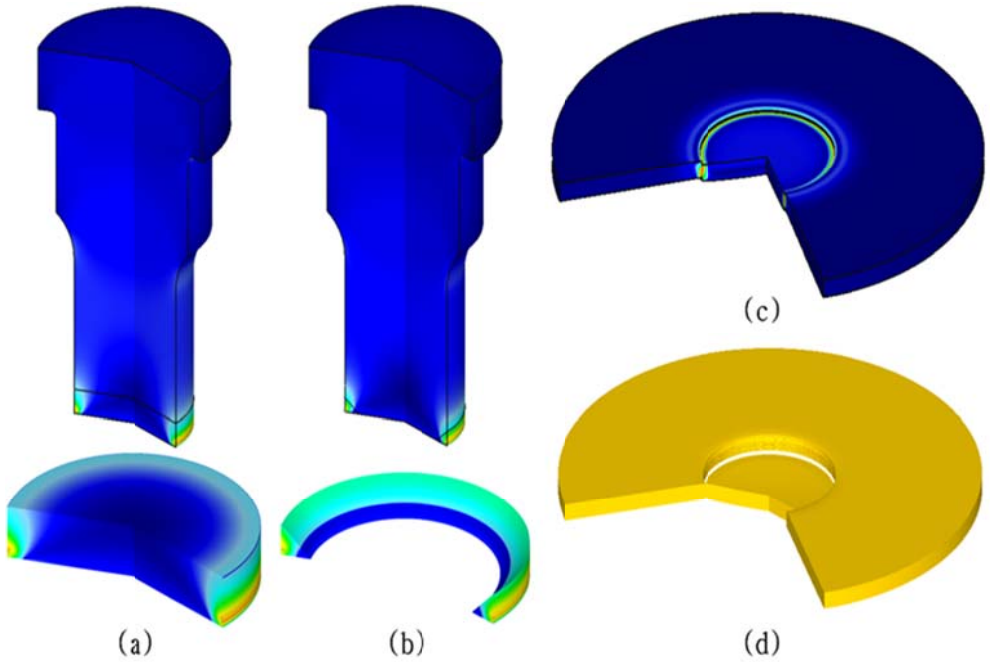

Fig. 6.4 Simulation results: (a) (b) Stress distribution of the semi-additive punch, (c) Stress distribution of the shear sheet material, (d) Shear shape of sheet material

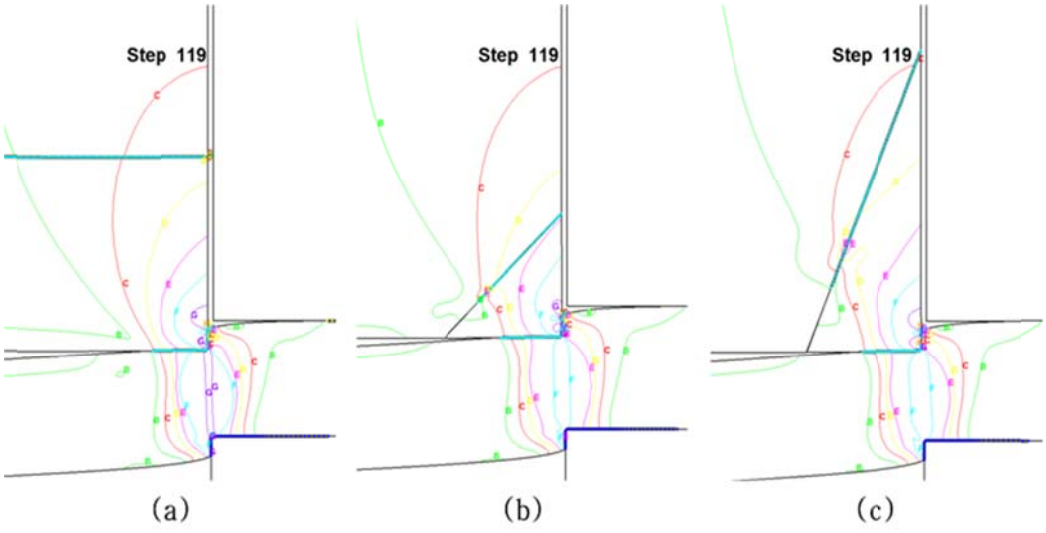

Fig. 6.5 Simulation results: (a) Stress distribution contour line of the plate shape type, (b) Stress distribution contour line of the equilateral triangle shape type, (c) Stress distribution contour line of the right triangle shape type

In the simulation analysis of this semi-additive shape selection, the stability at the joint interface was indirectly judged by comparing the damage value which acts on the sheet material according to the designed shape analysis. The range of stress distribution, the slip and peel state at the interface, the size of the stacking range, and the difficulty of additive were defined as criteria for the selection of shapes. Figure 6.6 shows the results of the analysis. Figure 6.7 shows examples of slip and separation at the interface. As shown in Figure 6.6, it can be seen that change of the damage value shows a relatively smooth curve tendency as compared with other shapes. However, the change of the damage value is greatly observed in other shapes. It seems that the influence of the slip and the bending moment depend on the shape and size of the joint interface which affects instantaneous damage value. The sudden increase of the damage value in a small stroke seems to be a temporary increase in the damage value at the corner contact portion due to the separation and bending moment. It is considered that the small value of the damage value at the large stroke is the influence of slip.

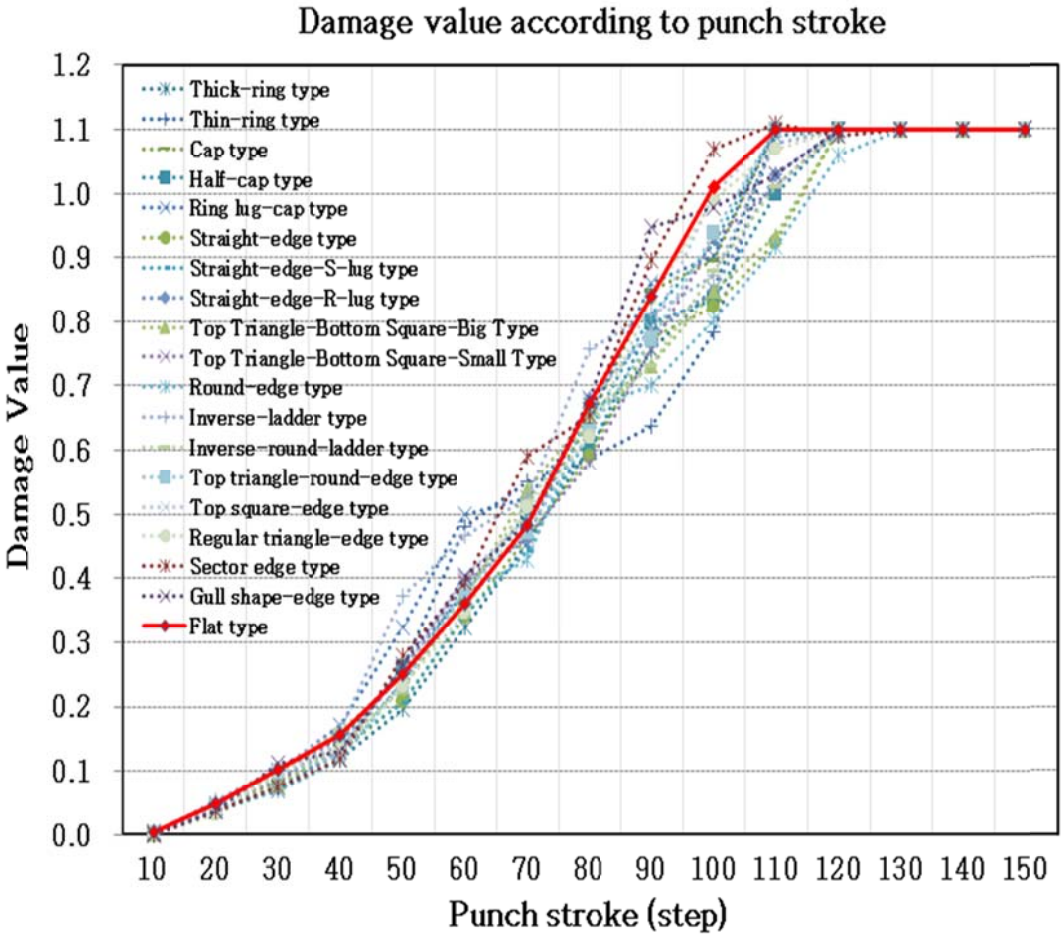

Fig. 6.6 Comparison of sheet material damage values by semi-additive shape

As mentioned above, the shape of the flat type is the most stable. Next, the edge shape with a triangular cross section is stable. It means that in a semi-additive configuration, the interface is more stable when it has a 45-degree interface rather than a vertical and acute-angled configuration. An example of such a phenomenon is summarized from the results of simulation analysis.

Figure 6.7 (a) and (b) show that the cross-sectional size of the equilateral triangular cross section with 45-degree interface does not affect the slip. The size of the cross section did not affect slip, but it affected the degree of separation. Figure 6.7 (c) shows the case of a triangular cross-section with acute interface, which is more susceptible to slip than the equilateral triangular cross-section. Figure 6.7 (d) shows a case where the interface is curved.

It is found to be both vulnerable to flake and slip. Therefore, it is more stable to have an isosceles triangle section than an acute angle triangle section. Also, it is shown that the interface composed of pure lines is more stable. Figure 6.7 (e) and (f) show the case of the ring type which has a rectangular cross section with a vertical interface. As the interface moves away from the punch blade, the phenomenon of separation becomes large and No sliding occurs. And there is a phenomenon that a step is generated. Therefore, in the case of the ring-shaped Additive shape, it considered to be advantageous to reduce the separation, if possible, to Additive as thin as possible in the depth direction of the punch body.

The most stable shape of the semi-additive shape was a simple plate type. There is no slip or separation phenomenon occurred at the additive interface. The sheer force of the punch is stably transmitted to the material so that the stress distribution is in the shape of the punch of the same material, and the same tendency is observed. It was confirmed that the corner edge of the punch was partially or vertically machined to cause warping due to separation, slip phenomenon and the additive shape at the interface. Particularly, it was found that the separation occurred more in the shape having the interface near the vertical, and the slope was more influenced by the slant angle closer to an acute angle. Therefore, in the case of a ring type of additive shape, it is considered to be advantageous to reduce the separation as thin as possible in the depth direction of the stamped body.

In this study, there is a design of a partial semi-additive shape for reinforcing punching strength which is aimed at minimizing the stacking capacity and minimized the stacking time for high-priced high-strength powder. However, because of the limited range, the purpose of overcoming the limit of the shape range is to be larger in the case of additive manufacturing high-strength metal steel. On the other hand, the range of strengthening the mold is small when the range of additive is not large like the piercing punch. It may be disadvantageous in

terms of cost rather than the advantage of strengthening the gold by processing the punch blade part into a complicated shape. It is advantageous to select a simple shape that can reduce the punch body machining and facilitate the stacking as much as possible in the case of this semi-additive shape selection study. For this purpose, it is necessary to excavate high-strength powder which can be desired range without any restrictions on the range.

As shown in this research, the results obtained from the analysis of the various semi-additive shapes presented to absorb the impact force acting on the punches. It was analyzed to be susceptible to impacts as the shape was complicated. The results of the analysis show that the stress is maximized at the beginning of shearing. The stress concentration is at the punch edge and the side of the punch. Therefore, in the semi-additive for punch reinforcement will be a means to increase the life of the punch. The area of additive as thin as possible would be a means of increasing life.

Through this study, the selected semi-additive shape will be used in fabricating partially semi-additive punch using 3D printing of AM DED technology. And it will be validated through durability test in hot stamping process of high strength automobile parts production line.

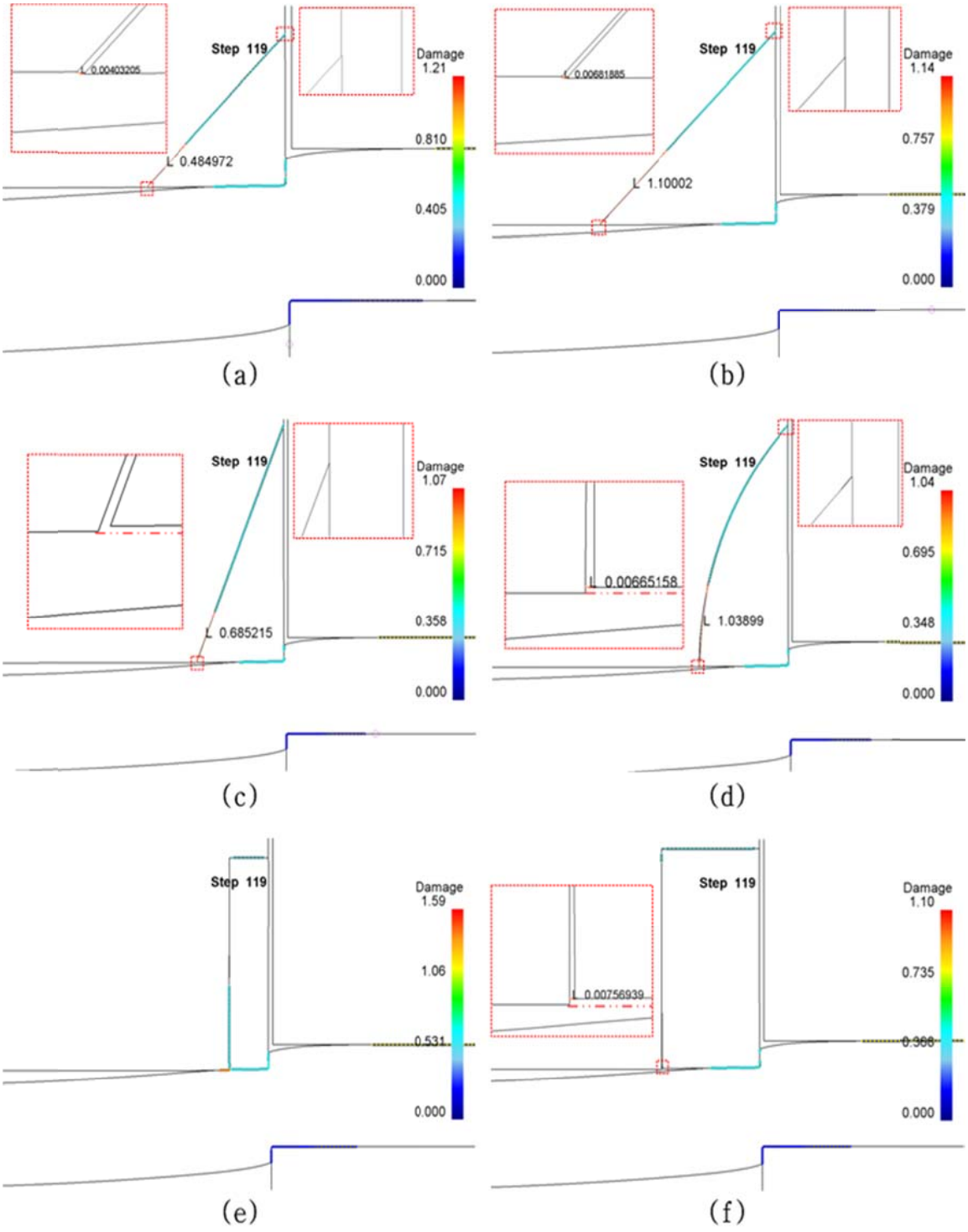

Fig. 6.7 Example of slip and separation at the contact interface

6.3 The summary of the predication of the shape

In the selection of the semi-additive shape, the shape of the flat type was found to be the most stable to the next the shape of the edge having the triangular sectional shape was found to be stable. The boundary with pure line is more stable than the case with 45 degree boundary and the case with curve. In the shape of a rectangular cross section having a vertical interface in this semi-additive shape selection, as the interface moves away from the punch edge, separation phenomenon may occur. Therefore it is advantageous if it is possible to additive thinly in the depth direction of the punch body. In the selection of the semi-additive shape, the more complex the shape, the more susceptible to impact, and the larger the additive area, the more slip or separation easily occurs.

6.4 The fabrication of the semi-additive punch

Based on the previous experiments and analysis, the process of semi-additive manufacturing punch was finally determined as shown in the flow chart.

STEP 1: Shape prediction

- Semi-Additive shape design

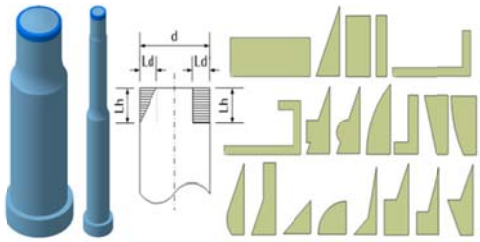

- Analysis software: DEFOR

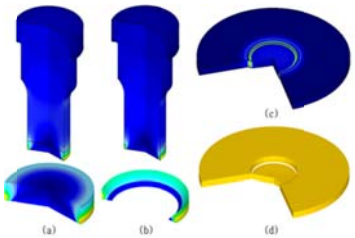

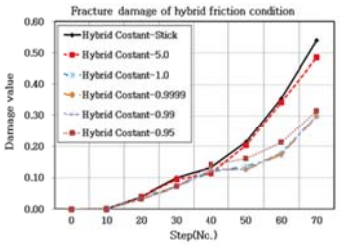

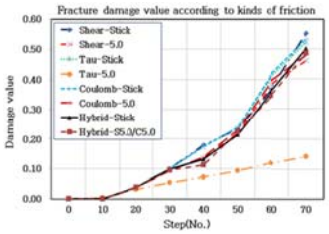

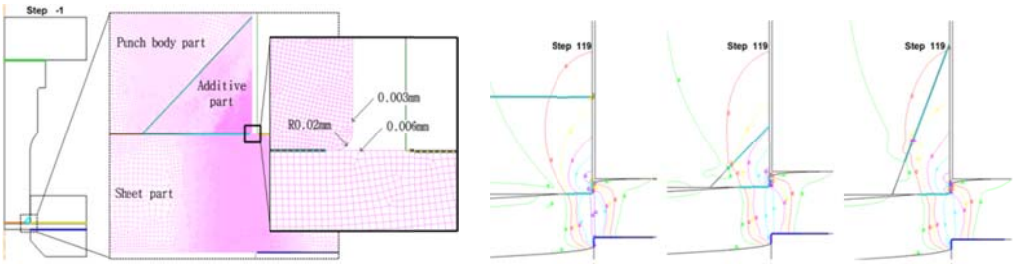

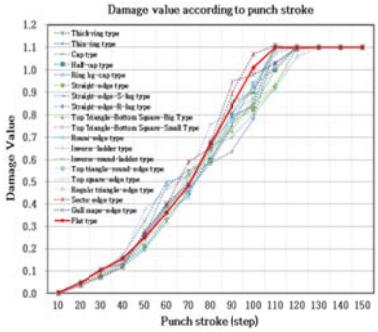

- Result

The shape of the flat type was found to be the most stable.

STEP 2: Material

- Chemical compositions of HWS powder

Powder	C	Si	Mn	P	S	Ni	Cr	Mo	Cu	V	W
HWS	1.08	1.38	0.34	-	-	-	7.80	1.86	-	2.66	1.73

- SEM of HWS

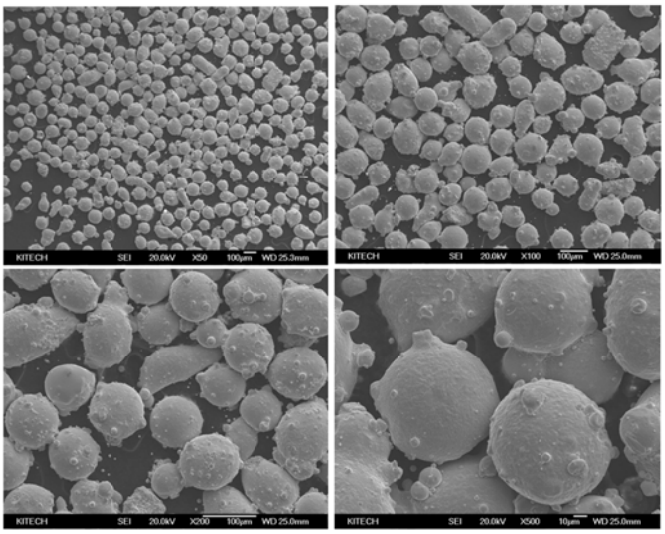

- On average 80-160μm powder is the mostly distributed
- The shape analysis of 5000 samples of HWS showed that the powder was close to spherical.

STEP 3: Additive manufacturing method

- Directed Energy Deposition (DED)

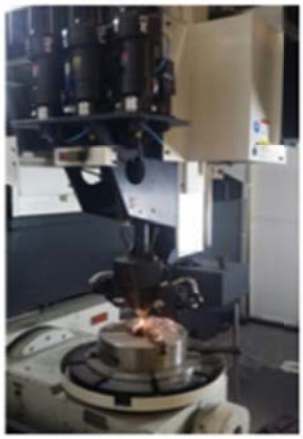

- DED equipment is developing from DMT (Direct Metal Tooling) MX3 metal printing equipment developed by Insstek (Korea) Co., Ltd.

- Parameters for DED processing

Laser power (W)	800
Slicing layer height (mm)	0.25
Overlap spacing(mm)	0.5
Powder feeding rate (g/mm)	5
Substrate traverse speed (mm/min)	850
Powder gas (ℓ/min)	2.5
Coaxial gas (ℓ/min)	8.0

STEP 4: Fabrication of Semi-additive punch

- Semi-additive manufacturing punch

AM part material	HWS
Punch body material	bulk D2
AM method	DED
Semi-additive shape	flat type

Chapter 7 Conclusion

In this paper, there was a comparison and analysis of the additive manufacturing technology which included DED, PBF and other additive manufacturing methods. The result showed that DED technology is more suitable for partial additive manufacturing. HWS additive manufacturing powder metal materials showed good properties after particle analysis. Then the additive manufacturing specimens fabricated by DED method and HWS powder material. The experiment was been setup including hardness test, Charpy impact test, compression test, wear test and true density test. The test specimens were designed according to the test standards, and the analysis of the test procedures and results were also strictly in accordance with the standard. For the test results, the mechanical properties of additive manufacturing specimens are already close to bulk materials.

Then, the shape prediction of the semi-additive punch was performed. The range (depth / height) of the semi-additive shape predicted in this study is within the range of 2 to 3 mm. According this range, various shapes were designed to get the optimal solution. In the selection of the semi-additive shape, the shape of the flat type was found to be the most stable, and the shape of the edge having the triangular sectional shape was found to be stable. Finally, two semi-additive punches were fabricated successfully.

In this project, the first reward is familiar with the background technology of 3D printing technique for the additive manufacturing especially in the knowledge of DED (Directed energy deposition) technology and PBF (Powder Bed Fusion). Secondly, there is also a profound study of the current state of powder materials like the mold steel and high speed tool steel. The analysis of additive manufacturing powder metal materials include the average particle size and particle size distribution of the powder, true density of the powder, the shape of the particles, and the microstructure. Then, in the experimental part, the test

standard is the basis. The solution to the problem and the analysis of the results during the test is an indispensable part. Finally, the application of software let me know the importance of simulation. A more comprehensive engineering analysis capability is my next goal.

For the future work, two different size of semi-additive punched will be performed for the durability test in order to validate the application. Then it will be combining with different software to analyze additive manufacturing process. More metal powder material and additive manufacturing methods will be applied. During the experimental analysis phase, analysis like SEM and EDS will be added in research. Finally, it is necessary to improve the toughness of the HWS powder by additive manufacturing the powder with excellent toughness as an intermediate layer.

REFERENCE

[1] Benteler AG (2006) Picture library, Germany.

[2] Rogelio Perez-Santiago, Eren Billur, Agim Ademaj, Carlos Sarmiento, Rodrigo Berlanga and Taylan Altan, “Hot Stamping a B-Pillar with Tailored Properties: Experiments and Preliminary Simulation Results”, Hot Stamping Conferences, Lulea, Sweden, June 2013

[3] Young Jin Yum, Soon Yong Yang, Yong Seok Kim, Hoang Van Tho, Jin Young Kim, Seong Woong Choi and Jong Won Kum “A Study on the Fabrication of Punch for the Post Processing of Ultra High Strength Part by Hot Stamping Using 3D Printing Technology,” The Korean Society of Mechanical Engineers. pp. 307-308, April 2017.

[4] Woo-Sung Kim, Myung-Pyo Hong, Jun-Seok Park, Yun-Soon Lee, Kyoung Je Cha, Ji-Hyun Sung, Min-Wha Jung, Ye-Hwan Lee,“Case Studies on Applications of Conformal Cooling Channel Based On DMT Technology,” Journal of the Korean Society of Manufacturing Process Engineers, vol.14 No.3, pp.9-14, June 2015.

[5] W. Kim, M. Hong, Y. Kim, C. H. Suh, J. Lee, S. Lee, and J. H. Sung, “Effects and Application Cases of Injection Molds by using DED type Additive Manufacturing Process,” Journal of Welding and Joining, vol. 32, no. 4, pp. 10–14, Aug. 2014.

[6] M. P. Hong, J. H. Sung, D. C. Ahn, Y. S. Kim, “A Study on Three-Dimensional Molding Technology Mold Directly How to Repair,” Proceedings of KSCE 2014 Spring Conference, pp. 247-249, May 2014.

[7] W.-S. Kim, M.-P. Hong, J.-S. Park, Y.-S. Lee, K. J. Cha, J.-H. Sung, M.-W. Jung, and Y.-H. Lee, “Case Studies on Applications of Conformal Cooling Channel Based On DMT Technology,” Journal of the Korean Society of Manufacturing Process Engineers, vol. 14, no. 3, pp. 9–14, Jun. 2015.

[8] W. Kim, M. Hong, Y. Kim, C. H. Suh, J. Lee, S. Lee, and J. H. Sung, “Effects and Application Cases of Injection Molds by using DED type Additive Manufacturing Process,” Journal of Welding and Joining, vol. 32, no. 4, pp. 10–14, Aug. 2014.

[9] G. Y. Baek, G. Y. Shin, E. M. Lee, D. S. Shim, K. Y. Lee, H.-S. Yoon, and M. H. Kim, “Mechanical characteristics of a tool steel layer deposited by using direct energy

deposition,” Metals and Materials International, vol. 23, no. 4, pp. 770–777, Jul. 2017.

[10] D.-S. Shim, G.-Y. Baek, and E.-M. Lee, Effect of substrate preheating by induction heater on direct energy deposition of AISI M4 powder, Materials Science and Engineering, (2017)550–562.

[11] M. Pleterski, T. Muhič, B. Podgornik, and J. Tušek, “Blanking punch life improvement by laser cladding,” Engineering Failure Analysis, vol. 18, no. 6, pp. 1527–1537, Sep. 2011.

[12] J. S. Park, M.-G. Lee, Y.-J. Cho, J. H. Sung, M.-S. Jeong, S.-K. Lee, Y.-J. Choi, and D. H. Kim, “Effect of heat treatment on the characteristics of tool steel deposited by the directed energy deposition process,” Metals and Materials International, vol. 22, no. 1, pp. 143–147, Jan. 2016.

[13] D. L. Bourell, D. W. Rosen, and M. C. Leu, “The Roadmap for Additive Manufacturing and Its Impact,” 3D Printing and Additive Manufacturing, vol. 1, no. 1, pp. 6–9, Mar. 2014.

[14] Y. S. Kim, R. Li, V. T. Hoang, J. W. Kum, Y. J. Yum, S. Y. Yang, “A Study on the Production of Full-Additive Manufacturing Punch fabricated of High-Strength Mold Steel Powder Materials Using 3DP Technique,” 21st International Conference on Mechatronics Technology, pp.366–371, Oct. 2017.

[15] R. Li, V. T. Hoang, J. W. Kum, Y. S. Kim, Y. J. Yum, S. Y. Yang, “A Study on the Prediction of Punch Shape Range for Improving Punch Strength by Partial Semi-Additive Method Using Metal 3D Printing Technique,” 21st International Conference on Mechatronics Technology, pp.350–354, Oct. 2017.

[16] R. Li, Y. S. Kim, V. T. Hoang, Y. J. Yum, W. J. Kim, S. Y. Yang, “A Study on the Additive Manufacturing (AM) of Piercing Punch by the PBF Method of Metal 3D Printing Using the Mold Steel Powder Materials,” Journal of Mechanical Science and Technology, Unpublished, 2018.

[17] I. Gibson, D. Rosen, and B. Stucker, “Directed Energy Deposition Processes,” Additive Manufacturing Technologies, pp. 245–268, 2015.

[18] F. Caiazzo and V. Alfieri, “Laser-Aided Directed Energy Deposition of Steel Powder over Flat Surfaces and Edges,” Materials, vol. 11, no. 3, p. 435, Mar. 2018.

[19] I. Gibson, D. W. Rosen, and B. Stucker, “Powder Bed Fusion Processes,” Additive Manufacturing Technologies, pp. 120–159, 2010.

[20] M. Taufik and P. K. Jain, “Role of build orientation in layered manufacturing: a review,” International Journal of Manufacturing Technology and Management, vol. 27, no. 1/2/3, p. 47, 2013.

[21] Mincheol Kang, “The Strategic Opportunities of Metal Powder and Applications for an Additive Manufacturing Age,” 3D Printing Research Association, Document of invitation seminar for metal 3D printing specialists of UOU, 2016.

[22] ASTM E9-89a: Standard Test Methods of Compression Testing of Metallic Materials at Room Temperature

[23] ASTM E23: Standard Test Methods for Notched Bar Impact Testing of Metallic Materials

[24] ASTM Standard Test Method E384: Standard Test Method for Microindentation Hardness of Materials

CONFERENCES

1. R. Li, V. T. Hoang, J. W. Kum, Y. S. Kim, Y. J. Yum, S. Y. Yang, “A Study on the Production of Full-Additive Manufacturing Punch Fabricated of High-Strength Mold Steel Powder Materials Using 3DP Technique,” 21st International Conference on Mechatronics Technology, pp.366–371, Oct. 2017.

2. R. Li, V. T. Hoang, J. W. Kum, Y. S. Kim, Y. J. Yum, S. Y. Yang, “A Study on the Prediction of Punch Shape Range for Improving Punch Strength by Partial Semi-Additive Method Using Metal 3D Printing Technique,” 21st International Conference on Mechatronics Technology, pp.350–354, Oct. 2017.

3. R. Li, V. T. Hoang, J. W. Kum, Y. S. Kim, Y. J. Yum, S. Y. Yang, “A Study on Analytical Prediction of Punch Strength Required for Ultra High Strength Parts in Piercing Process after Hot Stamping,” International Forum on Strategic Technology, Ulsan, Republic of Korea, May 2017.

4. R. Li, V. T. Hoang, J. W. Kum, Y. S. Kim, Y. J. Yum, S. Y. Yang, T. Gou, “A Study on Mechanical Properties of HWS (High Wear resistance Steel) Powder Material using the Additive Manufacturing (AM) DED (Directed Energy Deposition) Process by Metal 3D Printing,” International Forum on Strategic Technology, Harbin, China, May 2018.

5. R. Li, V. T. Hoang, J. W. Kum, Y. S. Kim, Y. J. Yum, S. Y. Yang, “A Study on the Semi-Additive Shape Design for High-strength Metal Molds of Functional Part by Using High Alloy Tool Steel (High Speed Steel) Powder and Metal 3D Printing Technique”, The Korean Society of Automotive Engineers Annual Autumn Conference and Exhibition, Gimhae, Republic of Korea, Oct. 2017.

6. R. Li, V. T. Hoang, J. W. Kum, Y. S. Kim, Y. J. Yum, S. Y. Yang, “A Study on the Additive Manufacturing(AM) of Piercing Punch by the PBF Method of Metal 3D Printing Using the Mold Steel Powder Materials,” The Korean Society of Manufacturing Technology Engineers, Jeju Island, Republic of Korea, Dec. 2017.

JOURNAL

1. A Study on the Additive Manufacturing (AM) of Piercing Punch by the PBF Method of Metal 3D Printing Using the Mold Steel Powder Materials-under review, Journal of Mechanical Science and Technology, 1738-494X (Print) 1976-3824 (Online), under review.

LIST OF PROJECT

번호	과제명	사업명	연구기간	참여기관
1	3D 프린팅 기법을 이용한 자동차 초고강도부품(1500MPa)용 컷팅 프로세스 및 핫스템핑 금형 개발 기초연구	지역신산업선도 인력양성사업	2016.06.01 ~2019.05.31	엠디티㈜
2	데이터처리율 향상을 위한 사물인터넷기반의 공정품질관리 시스템	산학공동기술 개발지원사업	2017.06.01 ~2018.05.31	ING KOREA
3	직교로봇용 2축(회전-틸팅) 증설 유닛 유효자세 분석	기타사업	2016.12.19 ~2017.02.18	모던테크

IFOST 2018

The 13th International Forum on Strategic Technology

CERTIFICATE
Excellent Paper Award

to

Rui Li, Yong Seok Kim, Van Tho Hoang, Young Jin Yum, Soon Yong Yang, Won Jun Kim, Tian Gou

of

University of Ulsan

This Best Paper Award is presented to you for your outstanding paper entitled:

A study on mechanical properties of HWS (high wear resistance steel) powder material using the additive manufacturing (AM) DED (directed energy deposition) process by metal 3d printing

which was presented at the 13th International Forum on Strategic Technology (IFOST 2018) May 30-June 1, 2018, Harbin, China.

IFOST

The 13th International Forum on Strategic Technology
IFOST 2018
Organizing Committee

Dayong Li
General Chair of
IFOST 2018
May 30-June 1, 2018
Harbin, China

CERTIFICATE

FOR BEST PAPER AWARD

of the 21st International Conference on Mechatronics Technology (ICMT2017)

conferred to

Li Rui, Van Tho Hoang, Jong Won Kum,
Yong Seok Kim, Young Jin Yum and Soon Yong Yang

for the paper entitled

A Study on the Prediction of Punch Shape Range for Improving Punch Strength by Partial Semi-Additive Method Using Metal 3D Printing Technique

Dr. Truong Quoc Thanh
General Chair, ICMT 2017